

# 2012 SNM Highlights Lectures

**F**rom the Newsline Editor: The Highlights Lecture, presented at the closing session of each SNM (now SNMII) Annual Meeting, was originated and presented for more than 33 y by Henry N. Wagner, Jr., MD. Beginning in 2010, the duties of summarizing selected significant presentations at the meeting were divided annually among 4 distinguished nuclear and molecular medicine subject-matter experts. The 2012 Highlights Lectures were delivered on June 13 at the SNM Annual Meeting in Miami, FL. The first 2 presentations are included here, and the remaining 2 will appear in the October issue of Newsline. Peter Herscovitch, MD, cochair of the Scientific Program Committee, introduced Frank Bengel, MD, and Satoshi Minoshima, MD, PhD, who spoke on cardiology and neurosciences, respectively. Note that in the following presentation summaries, numerals in brackets represent abstract numbers from The Journal of Nuclear Medicine (2012;53[*suppl 1*]).

## Cardiovascular Highlights

I began preparing for this presentation by thinking about definitions, an area in which perspective is key. If one looks up the definition of the word “heart,” for example, the dictionary describes “a hollow, muscular organ which, by contracting rhythmically, keeps up the circulation of the blood.” A broader definition might say that the heart is “the chief or vital portion; the center of activity.” Perspective is also key in defining the increasingly complex activities associated with cardiovascular nuclear medicine. A somewhat dry definition might characterize it as “a frequently used application of radiotracers, for SPECT imaging of myocardial perfusion” (MP). A more enthusiastic and forward-looking perspective might assert that cardiovascular nuclear medicine is “a driving force for rapid and sustained development of the entire field.” Perspective plays a central role in many of the presentations at this meeting, and I will return to the importance of viewpoint later in this lecture.

Submissions for presentations in both the cardiovascular basic and clinical sciences grew in number this year, in line with submissions in other subject matter areas. This is evidence of the tremendous success of the meeting. We must look beyond quantity to assess the changing foci of these presentations. I compared this year’s presentations with those from 2007 and identified several interesting trends. In 2007, ~45% of all cardiovascular abstracts dealt with perfusion; in 2012 this percentage was 31%. In 2007, ~41% of presentations focused on molecular imaging, a percentage that rose to 48% in 2012. The percentage of presentations on new hardware and software rose from 14% to 21% over this 5-y period. Similar trends were also observed when looking at the relative contributions of SPECT and PET. In 2007, cardiovascular presentations were dominated by SPECT at 56% (with 9% SPECT/CT and 1% cadmium-zinc-telluride (CZT)-based cameras), with PET at 44% (and no PET/MR). This year PET and SPECT each constituted about 50% of presentations, with 2% of these focusing on PET/MR, 6% on SPECT/CT, and 5% on CZT-based cameras.

## Myocardial Perfusion Imaging

In SPECT imaging, the current focus is clearly on lowering dose. DePuey et al. from St. Luke’s-Roosevelt Hospital and Columbia University (New York, NY) reported on “Five-mCi MP SPECT with a conventional NaI camera” [1792]. They obtained high-quality MP studies with a wide-beam resolution recovery reconstruction algorithm. They were able to obtain good images (Fig. 1). In cases of inferior image quality they found that extending acquisition

time and repeating the imaging yielded results that were sufficiently informative to allow stress-only MP imaging, without the rest study.

A number of submissions on MP imaging focused on PET technologies and absolute quantification of myocardial blood flow (MBF). We have seen the emergence of software algorithms that can now be used in the clinic. Tahari et al. from the Johns Hopkins School of Medicine (Baltimore, MD), the Technische Universität Munich (Germany), and Hannover Medical School (Germany) reported on “Determination of absolute myocardial flow quantification: comparison of different software packages and methods” [32]. They compared 3 of these algorithms (Corridor4DM, a fractional anisotropy-based compartment model; FlowQuant, a region of interest [ROI]-based compartment model; and Munich Heart, an ROI-based retention model) and identified subtle differences in absolute flow measurement in  $^{82}\text{Rb}$  PET studies. Coronary flow reserve (CFR), however, was quite comparable using these algorithms.

In a large study, Murthy et al. from the Brigham & Women’s Hospital (Boston, MA) and the Cleveland Clinic (OH) reported on “Coronary vascular dysfunction and prognosis in patients age 75 and older” [22]. These authors looked at global CFR in clinical patients referred for MP PET/CT imaging. They found that patients older than 75 y in whom regional perfusion abnormalities could not be identified but whose global CFR was reduced to ( $<1.9$ ) had much higher cardiovascular mortality than an age-matched general population or an age-matched population with higher CFR ( $\geq1.9$ ).

Nkoulou et al. from University Hospital Zurich (Switzerland) reported on “Prognostic value of regional CFR in patients with fixed perfusion defects by ammonia MP PET” [247]. The study included 128 patients with fixed perfusion defects (i.e., myocardial infarction [MI]) who did not have regional myocardial ischemia (Fig. 2). Of interest, reductions in flow reserve in the noninfarcted remote area in these patients were associated with impaired outcomes and a higher rate of cardiovascular mortality.

Danad et al. from the VU University Medical Center (Amsterdam, The Netherlands) and Uppsala University (Sweden) also used quantitative flow measurements with PET/CT and combined these measurements with quantitative MBF under vasodilator conditions with CT coronary angiography (CTCA) obtained in the same imaging session. Their presentation was titled ‘Hybrid quantita-



**Frank M. Bengel, MD**

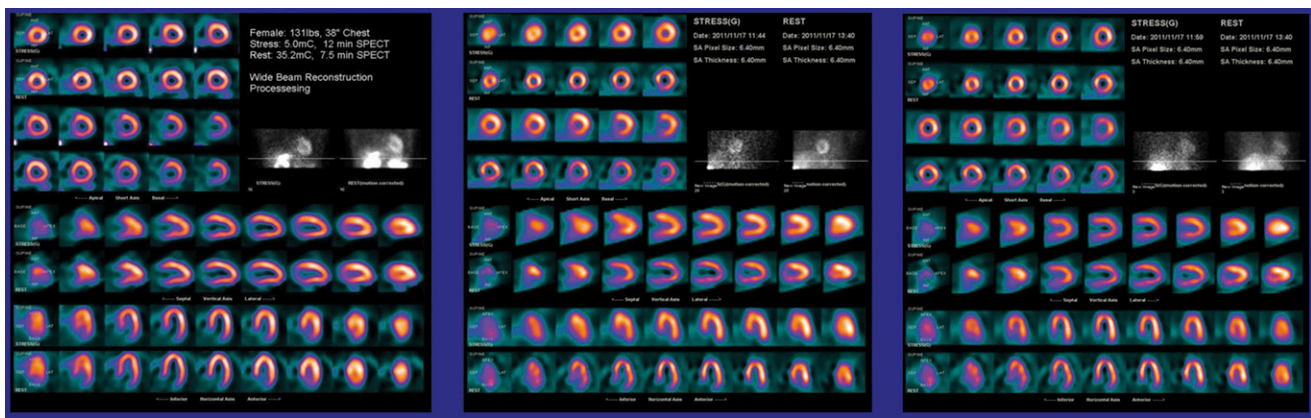


**FIGURE 1.** Five-mCi stress/32-mCi rest SPECT images processed with reduced count density wide-beam reconstruction (WBR) processing software. Left: Excellent stress and rest quality in study with 12-min stress SPECT and 7.5-min rest SPECT. Middle: Fair results in 12-min stress with WBR in another patient. Right: Excellent results with 16-min stress with WBR in same patient in middle image.

tive H<sub>2</sub><sup>15</sup>O PET/CT imaging for the detection of coronary artery disease” [244]. They were able to show that the combination of data from both PET/CT and CTCA resulted in higher accuracy in predicting the presence of coronary artery disease than CTCA, PET, or PET/CT alone.

In summary, a review of MPI highlights at the meeting indicates that: (1) In SPECT, the focus is on dose reduction. (2) PET continues to penetrate the clinical arena. (3) A strong focus on absolute

quantification of MBF is making such assessment a practical clinical reality. (4) We must wait to learn more about the directions that integrated assessment of coronary anatomy and perfusion will take in the future—only a few presentations touched on this topic.

## Cardiovascular Molecular Imaging

Myocardial viability assessment is perhaps the oldest molecular cardiovascular imaging application. This technique is still quite viable, as shown by Uebelis et al. from the University of Munich (Germany) and Cedars-Sinai Medical Center/University

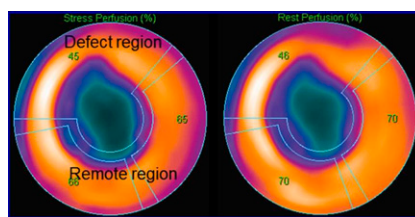


**FIGURE 2.** Stress (top) and rest (bottom) N<sup>13</sup>-ammonia PET MP images in a patient with a fixed perfusion defect but no myocardial ischemia.

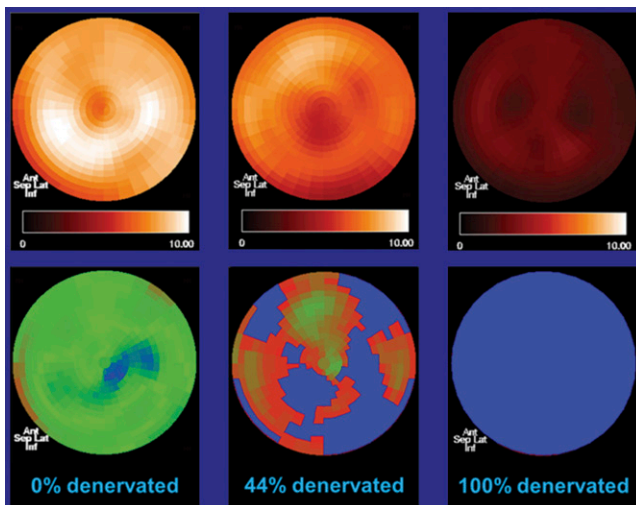


**FIGURE 3.** <sup>11</sup>C-hydroxyephedrine PET results in healthy subject (left) and patients (middle and right) with Parkinsonian syndrome. Top row depicts tracer retention. Bottom row depicts Z-scores. Left: 0% denervation in healthy individual. Middle: 44% (partial) denervation. Right: 100% (complete) denervation. In this study complete denervation was seen only in patients with idiopathic Parkinson disease (13 of 27) and not in patients with atypical syndromes such as multiple system atrophy (0 of 13).

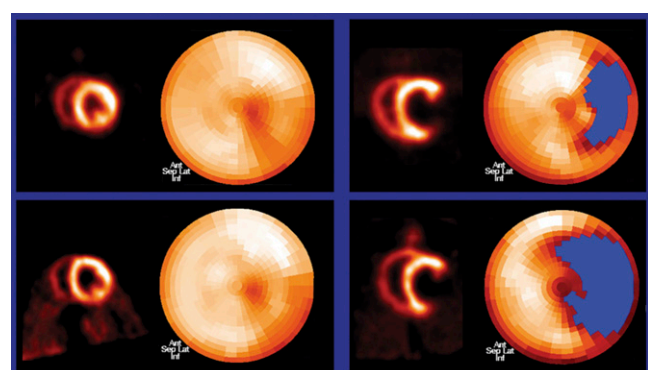


**FIGURE 4.** PET imaging of cardiac innervation and perfusion mismatch after MI in rabbits after ischemia-reperfusion injury. Top row: <sup>18</sup>F-flurpiradaz PET images. Bottom row: LMI1195 PET images. Left: short-axis and polar maps in control rabbit. Right: Corresponding maps at wk 4 after MI. Blue areas = defects, with <sup>18</sup>F-flurpiradaz (top) depicting perfusion defect and LMI1195 (bottom) depicting innervation defect.

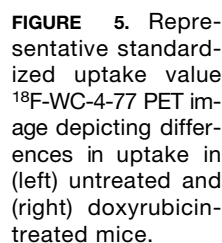


**FIGURE 5.** Representative standardised uptake value <sup>18</sup>F-WC-4-77 PET image depicting differences in uptake in (left) untreated and (right) doxorubicin-treated mice.

(Continued on page 18N)

(Continued from page 16N)

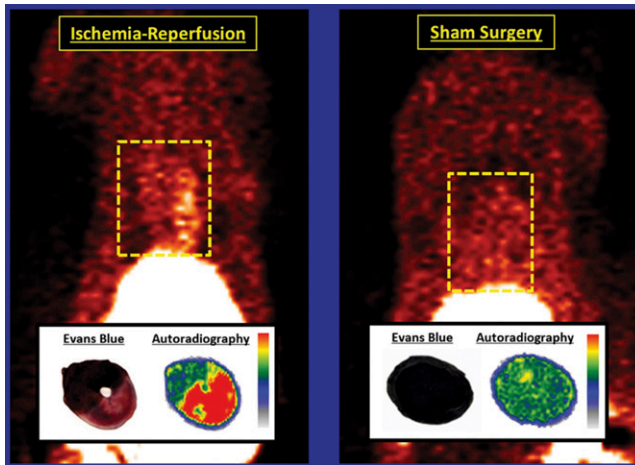


**FIGURE 6.**  $^{18}\text{F}$ -WC-4-116 PET imaging in rats after ischemia-reperfusion (left) and sham surgery (right). Insets show result of Evans Blue staining and autoradiography.

of California at Los Angeles, who reported on “MP SPECT in conjunction with  $^{18}\text{F}$ -FDG PET in the prediction of long-term survival in patients with ischemic cardiomyopathy and left ventricular [LV] dysfunction: the effect of early revascularization” [1863]. These researchers showed that a threshold of  $\geq 5\%$  SPECT/PET perfusion/metabolism mismatch predicted best which patients with ischemic cardiomyopathy and LV dysfunction would benefit from early revascularization in terms of long-term survival.

Myocardial innervation imaging is also increasingly penetrating the clinical arena. In Japan, it is already an accepted clinical procedure. Nakajima et al. from Kanazawa University Hospital, Sapporo Medical University, Toho University Medical Center, Cardiovascular Hospital of Central Japan, Osaka Prefectural General Hospital, Tokyo Women’s Medical University, and Shiga University of Medical Science (all in Japan) and GE Healthcare (Princeton, NJ) reported on “ $^{123}\text{I}$ -MIBG meta analysis for predicting cardiac death in heart failure: multicenter investigation in Japan” [87]. The study included 1,322 patients with heart failure. Results showed that a reduced heart/mediastinum ratio is associated with adverse cardiovascular outcomes and is indeed an independent predictor in a multivariate analysis.

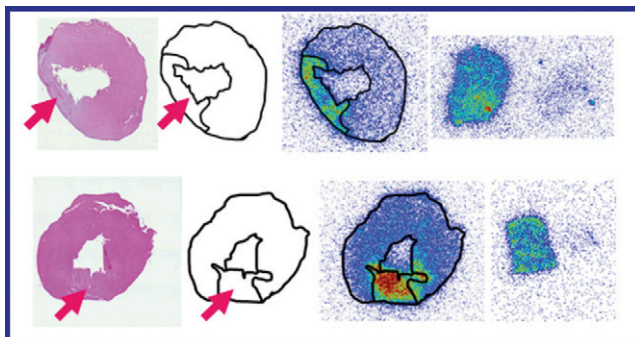


**FIGURE 7.** Evaluating  $^{68}\text{Ga}$ -labeled RGD peptides for  $\alpha_v\beta_3$  integrin detection in a rat model of MI. Top row:  $^{68}\text{Ga}$ -NODAGA RGD. Bottom row:  $^{68}\text{Ga}$ -TRAP(RGD)<sub>3</sub>. Left to right: hematoxylin and eosin-stained heart sections, infarct areas, and autoradiograms showing uptake in heart, muscle, and spleen.

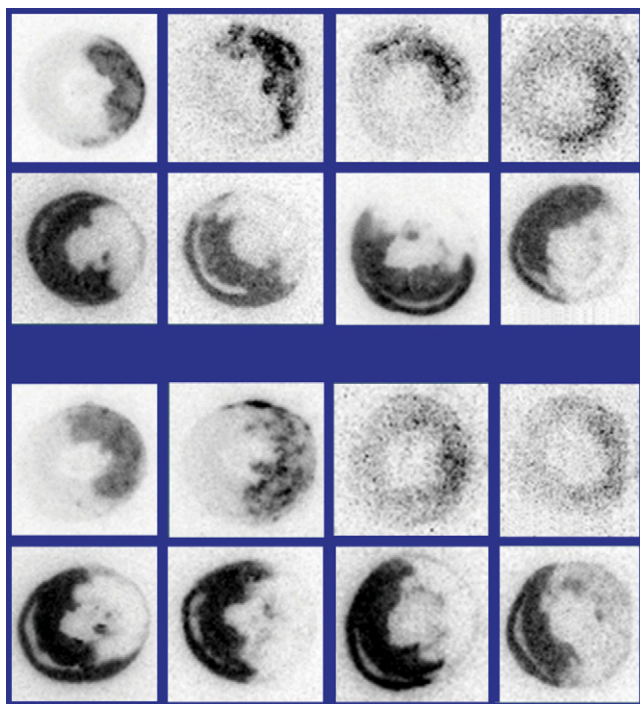


**FIGURE 8.**  $^{125}\text{I}$ -anti-tenascin-C-Ab uptake in rats after ischemia-reperfusion. Time period after reperfusion, left to right: 1, 3, 7, and 14 d. Top 2 rows: Control rats (without preconditioning) imaged with  $^{125}\text{I}$ -anti-tenascin-C-Ab (top) and  $^{99m}\text{Tc}$ -MIBI (bottom, area at risk). Bottom 2 rows: Postconditioned rats imaged with  $^{125}\text{I}$ -anti-tenascin-C-Ab (top) and  $^{99m}\text{Tc}$ -MIBI (bottom, area at risk).

Namazian et al. from the Hannover Medical School and the Technische Universität Munich (both in Germany) reported on “PET-defined myocardial sympathetic denervation in Parkinson syndromes: clinical correlates and impact on survival” [33] (Fig. 3). The researchers found that patients with Parkinsonian syndrome may have impaired innervation and that this is a function of increasing duration of the disease and ongoing neurodegeneration. However, at outcomes analysis the researchers were not able to identify prognostic value (unlike in cardiovascular disease) for the occurrence of cardiac events, which leads to the conclusion that primary (neurologic) damage of cardiac innervation has different implications for outcome than does secondary damage resulting from target organ disease of the heart.

Several groups are working on new tracers for cardiovascular innervation imaging. Kagan et al. from Lantheus Medical Imaging (North Billerica, MA) reported on “LMI1195 and flurpiridaz  $^{18}\text{F}$  PET imaging in evaluation of time-course changes in mismatch of cardiac denervated and perfusion defect areas following acute MI” [84]. In a rabbit model of MI at 4 wk after ischemia-reperfusion injury the authors showed that the innervation defect exceeded the perfusion defect area—in other words, some well-perfused areas may have poor innervation (Fig. 4). This may have implications for the presence of myocardial arrhythmia and for the development of heart failure later after MI.

Raffel et al. from the University of Michigan Medical School (Ann Arbor) continue to work on novel catecholaminergic tracers for cardiovascular imaging. They reported that “Patlak slope of  $^{11}\text{C}$ -guanyl-*meta*-octopamine kinetics in nonhuman primates tracks reductions in cardiac norepinephrine transporter densities”

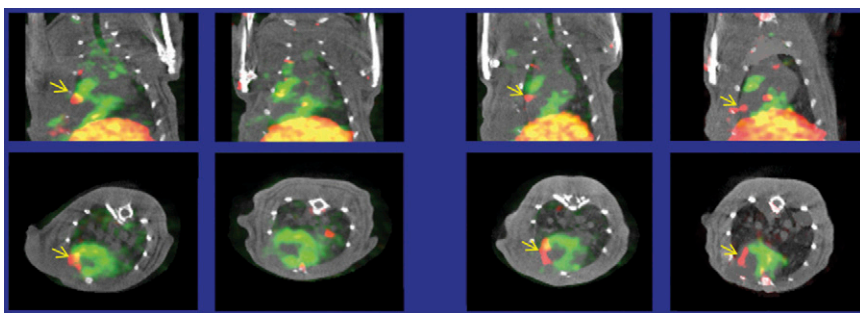
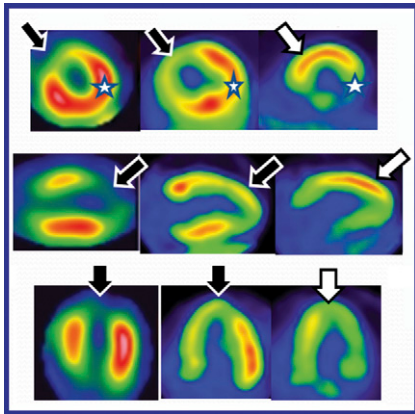


**FIGURE 9.** Dual-isotope  $^{99m}\text{Tc}$ -AN and  $^{201}\text{Ti}$  SPECT/CT imaging in rats after left anterior descending artery occlusion. Left: Coronal (top) and transverse (bottom) images at d 1 (left) and 7 (right) in rats treated with TGF- $\beta$ 1-conditioned human mesenchymal stem cell-laden fibrin patches. Right: Coronal (top) and transverse (bottom) images at d 1 (left) and 7 (right) in rats treated with an acellular (sham) patch.



tom row). Black arrows = decreased uptake. Stars in top row correlate with locations identified by arrows in remote areas.

[85]. This tracer shows slow uptake into sympathetic nerve terminals of the heart, so that it can be absolutely quantified using Patlak slope analysis. They were able to acquire robust measurements across a variety of different blocking conditions.

We have also seen a variety of novel agents targeting other molecular mechanisms in the heart. Apoptosis is one of those targets. Tamarappoo et al. from Siemens Molecular Imaging (Culver City, CA) and the Cleveland Clinic (OH) reported on “ $^{18}\text{F}$ -CP18, a novel PET tracer for detection of anthracycline-induced apoptosis and cardiotoxicity” [30]. This study was given the first-place Cardiovascular Council’s Young Investigator Award for Basic Science. The researchers demonstrated in their mouse model of anthracycline-induced cardiotoxicity that uptake of the

apoptosis tracer could be seen at 6 wk in doxorubicin-treated mice, weeks before contractile function actually declined. With such molecular tracers, we may be able to predict later occurrence of cardiovascular damage.

Shoghi et al. from the Washington University School of Medicine (St. Louis, MO) and the University of California, San Diego, worked with a similar animal model and reported on “PET imaging of reactive oxygen species” [26]. This group also showed that uptake of their tracer (WC477) was increased in doxorubicin-treated animals and seems to be a potential predictor of cardiotoxicity and damage to the myocardium (Fig. 5).

Thukkani et al. from the same group at Washington University School of Medicine reported on another apoptosis-targeting tracer in their presentation on “In vivo detection of myocardial caspase-3 activity utilizing the radiolabeled isatin analog  $^{18}\text{F}$ -WC-4-116” [34]. The focus in this case was on imaging damage after ischemia–reperfusion. The authors were successful in demonstrating both enhanced caspase-3 activity and  $^{18}\text{F}$ -WC-4-116 accumulation in the at-risk myocardium of ischemic–reperfused rats (Fig. 6). These results suggest that this is a good tracer for looking at the molecular mechanisms activated by MI.

Laitinen et al. from the Technische Universität Munich (Germany) looked at the accumulation of various RGD peptides in the infarcted myocardium in their report on “Evaluation of  $^{68}\text{Ga}$ -labeled RGD peptides for  $\alpha_v\beta_3$  integrin detection in MI” [460]. They were able to show that 2 different  $^{68}\text{Ga}$ -labeled peptides accumulate in the infarct area (Fig. 7). Their results indicated that expression of  $\alpha_v\beta_3$  integrin is decreased after MI as part of the repair process and can be imaged with the PET tracer  $^{18}\text{F}$ -galacto-RGD; that both  $^{68}\text{Ga}$ -NODAGA-RGD and  $^{68}\text{Ga}$ -TRAP(RGD)<sub>3</sub> are easily accessible and have high specificity, affinity, and high specific activity; and that uptake in in-

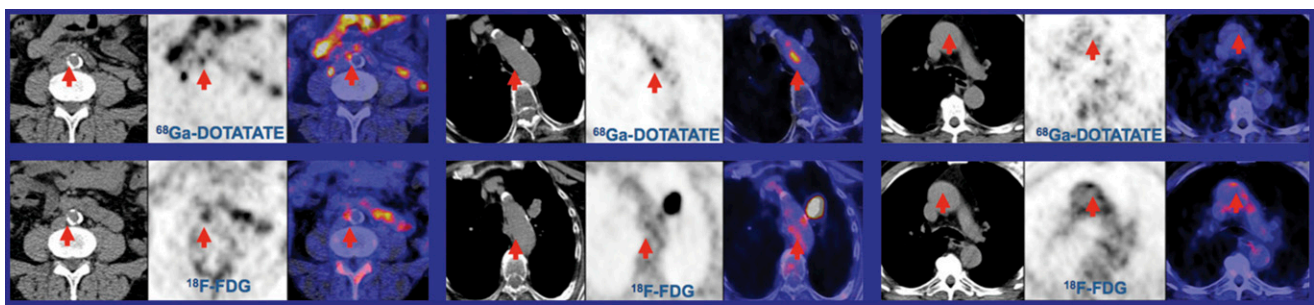


**FIGURE 11.**  $^{68}\text{Ga}$ -DOTATATE PET/CT (top row) and  $^{18}\text{F}$ -FDG PET/CT (bottom row) in cases of suspected inflammation in large arteries. Left block of 6 images: example of colocalization of the 2 tracers. Middle block: example with no colocalization, in which  $^{68}\text{Ga}$ -DOTATATE PET/CT was positive and  $^{18}\text{F}$ -FDG PET was negative. Right: example with no colocalization in which  $^{68}\text{Ga}$ -DOTATATE PET/CT was negative and  $^{18}\text{F}$ -FDG PET was positive.

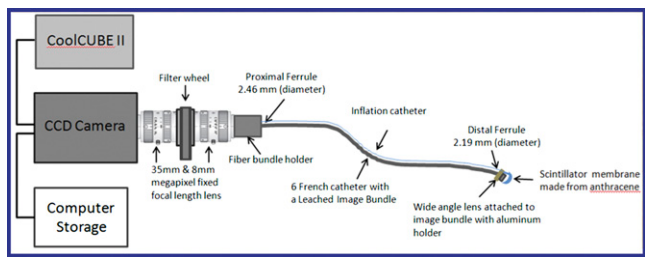


**FIGURE 12.** Catheter-based optical imaging system.

farct and remote areas in autoradiograms of MI-induced rats was correlated with the presence of CD31 (endothelial cells) and CD62 ( $\beta_3$  integrin). They concluded that because  $^{68}\text{Ga}$ -NODAGA-RGD and  $^{68}\text{Ga}$ -TRAP(RGD)<sub>3</sub> were equally able to detect the infarct defect area of rats at 1 wk after MI (comparable to  $^{18}\text{F}$ -galacto-RGD), these  $^{68}\text{Ga}$ -labeled RGD peptides show the potential to monitor repair mechanisms and angiogenesis after myocardial injury.

## Why is Acute MI a Primary Target for Molecular Imaging?

Various mechanisms are activated in the infarct area. We know that this activation defines later occurrence of LV remodeling; in other words, it predicts and predetermines the presence of heart failure. It also stimulates cell recruitment (inflammation, angiogenesis) and triggers myocardial regeneration. These mechanisms are increasingly serving as targets for novel therapeutic interventions.

Taki et al. from Kanazawa University (Japan), Mie University (Tsu, Japan), and the National Center for Global Health and Medicine (Tokyo, Japan) reported that "Postconditioning attenuates interstitial tissue remodeling in a rat model of severe ischemia and reperfusion: assessment of  $^{125}\text{I}$ -anti tenascin-C antibody imaging" [1762]. Their work showed that, with postconditioning, uptake of the tenascin-C antibody in the damaged infarct area was attenuated, suggesting that postconditioning may be a useful therapeutic intervention after ischemia reperfusion (Fig. 8).

In another very interesting study, Tekabe et al. from Columbia University (New York, NY) reported on "Noninvasive imaging of myocyte apoptosis following application of stem cell engineered delivery platform to acutely infarcted myocardium" [463]. The group used molecular imaging to measure the effects of an engineered tissue patch implanted onto the infarcted myocardium in rats. Initial cell culture experiments simulating engraftment of fibrin patches onto beating rat ventricular myocytes exposed to hypoxia showed

a response of reduced apoptosis in conditioned cells. Rats underwent left anterior descending artery occlusion and were divided into 3 groups: those with TGF- $\beta$ 1-conditioned human mesenchymal stem cell-laden fibrin patches, those with infarct alone without patch, and those with patch alone. At d 1 and 7, rats were injected with  $^{99\text{m}}\text{Tc}$ -AN and  $^{201}\text{Tl}$  and underwent dual-isotope SPECT/CT imaging (Fig. 9). Molecular imaging showed that in rats with TGF- $\beta$ 1-treated patches perfusion defect size was smaller and uptake of an apoptosis tracer was lower than in control animals, suggesting that molecular imaging can be used to characterize such highly sophisticated therapeutic interventions.

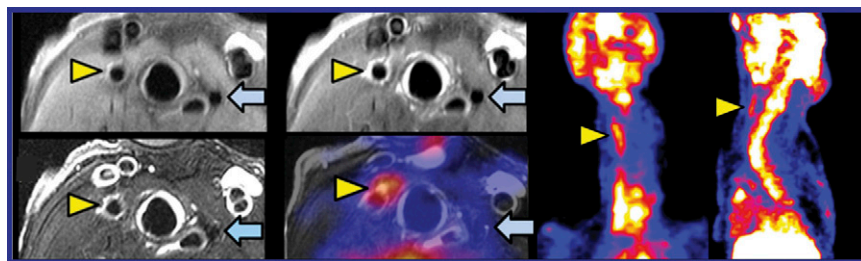
Some of these interventions are already being used clinically. Morooka et al. from the National Center for Global Health and Medicine (Tokyo, Japan) reported on "Myocardial inflammatory images:  $^{18}\text{F}$ -FDG PET/CT with heparin loading method in patients with acute MI" [1856]. They used heparin to suppress uptake in healthy myocardium and then observed increased FDG uptake in the hypoperfused infarct area early after infarct (Fig. 10). They also observed a correlation with peak white blood cell count in these patients, suggesting that it is feasible to image infarct inflammation *in vivo* in the human heart.

## Common Pathways

When assessing the injured myocardium, we must keep in mind the common pathways that unite such injuries with vulnerable plaque and with other situations outside the cardiovascular system, such as growing tumors. Many molecular mechanisms, such as glucose utilization, inflammation, angiogenesis, apoptosis, extracellular matrix activation, chemotaxis, and others are playing a role not only in the cardiovascular system but also in other organs and other diseases.

Li et al. from the Universitätsklinikum Würzburg (Germany) have taken a multitracer approach to assess focal vascular uptake and correlate it with calcium burden and cardiovascular disease risk factors in oncology patients. They reported on " $^{68}\text{Ga}$ -DOTATATE PET/CT for detection of inflammation of large arteries: correlation with  $^{18}\text{F}$ -FDG, calcium burden, and risk factors" [191].  $^{68}\text{Ga}$ -DOTATATE visualizes somatostatin receptor subtype-2 expressed on macrophages, and  $^{18}\text{F}$ -FDG is also known to be taken up in inflammatory vessel lesions and macrophages. Patients were divided into high- and low-risk groups. The researchers found that  $^{68}\text{Ga}$ -DOTATATE uptake correlated significantly with the presence of calcified plaques, hypertension, and age (Fig. 11). Uptake of  $^{18}\text{F}$ -FDG correlated significantly only with hypertension. Increased  $^{68}\text{Ga}$ -DOTATATE uptake therefore correlated more closely with known risk factors of cardiovascular disease than did  $^{18}\text{F}$ -FDG uptake, suggesting a potential role for

**FIGURE 13.** Atherosclerotic plaque imaging with PET/MR in a rabbit model. Left: Multicontrast MR TSE sequences show enhanced signal in injured carotid vessel wall (yellow arrowheads) but not in uninjured contralateral carotid (blue arrows). Middle: Fusion of T2W MR and PET data shows enhanced  $^{18}\text{F}$ -FDG uptake in injured carotid. Right: Coronal and sagittal PET views show tracer uptake localized to area of induced injury.



plaque imaging in large arteries. They also found that focal uptake of  $^{68}\text{Ga}$ -DOTATATE and  $^{18}\text{F}$ -FDG did not colocalize in a significant number of lesions.

At this meeting, Mehran M. Sadeghi, MD, from Yale University School of Medicine (New Haven, CT) received the Herrmann Blumgart Award, the most prestigious award of the Cardiovascular Council, and lectured on “Vascular molecular imaging: past, present, and future.” He summarized the range of different molecular tracers that can be used to assess various factors (calcification [ $\text{NaF}$ ]; endothelial activation [vascular cell adhesion molecule-1, P-selectin]; vascular smooth muscle cell proliferation/activation [ $\text{Z2D3}$ ,  $\alpha_v\beta_3$ ]; lipid core [oxidized low-density lipoproteins]; inflammation, including pH/temperature, cell trafficking and recruitment [labeled monocytes, chemokine receptors], phagocyte activity [nanoparticles], metabolism (FDG), integrin expression/activation [ $\alpha_v\beta_3$ ], and protease activity [matrix metalloproteinases, cathepsins]; apoptosis [annexin V]; and vasa vasorum/angiogenesis [ $\alpha_v\beta_3$ , vascular endothelial growth factor receptors]). Dr. Sadeghi also highlighted the many potential clinical applications in early atherosclerosis/atherosclerosis burden, plaque vulnerability, prediction of aneurysm rupture/dissection, vascular remodeling, transplant vasculopathy, restenosis, primary pulmonary hypertension, angiogenesis and arteriogenesis, stem cell and gene therapy, and others. He came to the conclusion that clinical vascular molecular imaging is possible and powerful, paradigm-shifting, and potentially effective. But he also pointed out that we will be required to demonstrate the incremental value of these techniques.

One of the ways we can get around the difficulties associated with a target as small as the vessel wall would be to use a system such as that discussed by Zaman et al. from the Stanford University School of Medicine (CA) in their presentation on “Development and quantification of a novel intravascular catheter-based radionuclide imaging system” [137]. Their optical imaging system (Fig. 12) includes a charge-coupled device camera paired with an imaging optical fiber bundle housed inside a catheter, with a filter wheel to capture FDG emissions at various wavelengths. The system converts the decay of FDG signal into light using a scintillating membrane. The group has performed *in vitro* studies with the system to identify the optimal scintillating membrane needed for high resolution and high sensitivity. We are all looking forward to *in vivo* applications of the system.

In summary, we are seeing that innervation will be, after viability imaging, next in a series of novel clinical molecular cardiovascular imaging targets. We are seeing that the inflamed infarct and vulnerable plaque are primary (and common) targets for development of novel probes and that the goals of molecular imaging in the heart include both prevention of progression and monitoring of specific interventions.

## New Cardiovascular Imaging Technology

We are seeing exciting developments in new technologies, as reflected at this meeting. Whole-body PET/MR is now also being applied for cardiovascular imaging. Zhang et al. from the Technische Universität Munich (Germany) reported on “First simultaneous measurement of MP on whole-body PET/MR” [29]. They showed that rest flow was comparable between the 2 modalities but that stress flow was depicted more accurately with the PET approach. They also showed

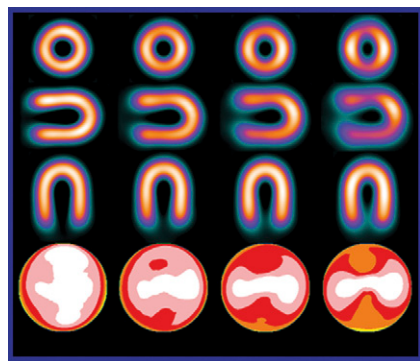


**FIGURE 14.** Phantom SPECT scans with different ranges of motion (left to right: 0, 15, 20, and 25 mm) using a CZT camera with list-mode acquisition.

nicely how to do intermodality cross-validation using this hybrid technology.

From members of the same group in Munich, Dregely et al. reported on using this PET/MR system in “Characterization of atherosclerotic plaques with simultaneous PET/MR: preliminary results in a rabbit model” [1759]. In exciting images (Fig. 13) they showed that that multicontrast MR TSE sequences enhanced signal in injured carotid vessel wall but not in uninjured, contralateral carotid. This enhanced signal could be colocalized with uptake on PET imaging in the same session. Such images and results in small experimental animals, obtained with a clinical PET/MR scanner, strongly support the strength of this new hybrid imaging system.

Ko et al. from the National Taiwan University Hospital (Taipei) and Far Eastern Memorial Hospital (New Taipei City, Taiwan) reported on “Effects of spontaneous respiration on MPI with CZT SPECT camera” [31]. This presentation won the Cardiovascular Clinical Young Investigator Award. The researchers made use of a novel solid-state camera that can acquire in list mode and showed in a phantom study that 15%–20% reduced activity may result from a 20-mm shift caused by respiratory motion. Based on these studies they developed a correction algorithm and looked at respiratory motion in clinical studies, where axial motion is not uncommon with CZT camera imaging, especially after treadmill stress. They were able to correct for potential artifacts in the clinical studies and obtained homogeneous myocardial distribution (Figs. 14 and 15).

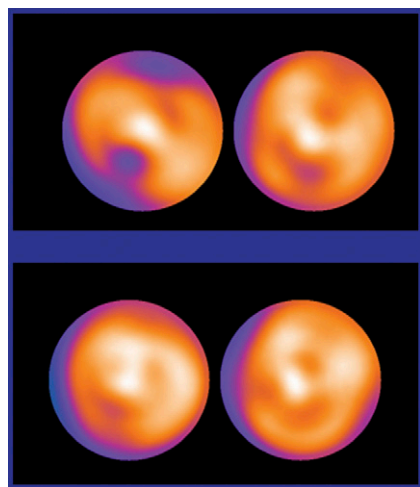
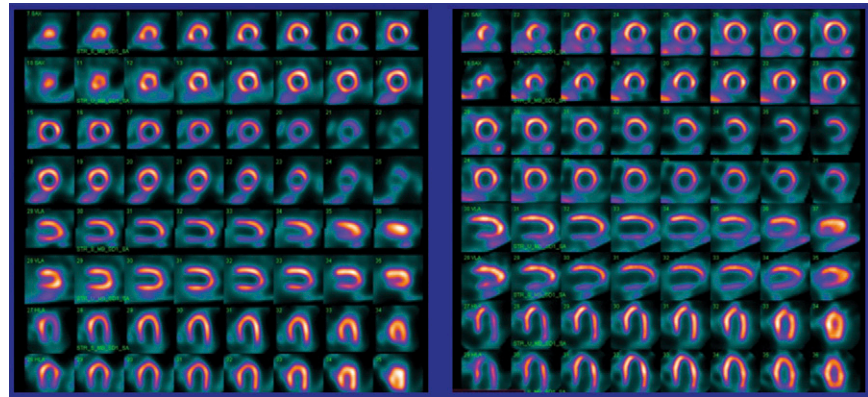


**FIGURE 15.** Polar maps from study in 42-y-old man with chest pain, with the same CZT camera in Fig. 14. Top row: Original poststress (left) and redistribution (right) images. Bottom row: Corresponding images after motion compensation.

**FIGURE 16.** MPI in overweight patients. Left: 64-y-old man with angina; body mass index (BMI) of 35. Previous angiogram showed mild left anterior descending artery (LAD) irregularity. Stress-only supine images (upper row) show inferior wall reduction. Upright images (lower row) show homogeneous inferior wall activity. Findings are consistent with artifact. Rest imaging may not be needed. Right: 50-y-old man; BMI of 36; previous MI and LAD and right coronary artery percutaneous intervention. Stress-only supine (upper row) and upright (lower row) images show persistent inferior wall reduction, consistent with true abnormality. Rest imaging is required.



Others are using this technique in the clinical setting. Ben-Haim et al. from University College London Hospitals (UK), Sheba Medical Center (Tel Hashomer, Israel), and Royal Victoria Hospital (Belfast, Ireland) reported on “Clinical value of supine and upright stress only MPI in overweight patients” [1807]. They found that when an inferior wall defect was present in the supine images but not in the upright images, the apparent defect was an artifact. If the defect was present on both images, it was not an artifact. They concluded that using the combined supine/upright imaging protocol stress-only MPI may be feasible in 58% of overweight patients. The additional upright imaging increased reviewers’ confidence in 73% of nondiagnostic or equivocal scans (Fig. 16). When applicable, stress-only MPI also enables a significant reduction in radiation exposure.

Others have made exciting use of these novel cameras, with dual-isotope simultaneous acquisition facilitated by high energy resolution. Kawaguchi et al. from Ehime University and the Gunma Prefectural College of Health Sciences (both in Japan) reported on “Feasibility of  $^{123}\text{I}$ -BMIPP and  $^{99\text{m}}\text{Tc}$ -tetrofosmin dual-isotope SPECT with dynamic acquisition using a fast gamma camera with CZT detector” [1775]. The 2 isotopes facilitated simultaneous imaging of molecular events and perfusion (Fig. 17).

In summary, many new technologies are being introduced and explored. Solid-state detectors have the potential to revolutionize SPECT because of their many advantages, including their stationary character, high sensitivity, and high energy resolution. And I believe that PET/MR, after it passes through its “childhood” phase, will experience a developmental boost from cardiovascular applications, which are usually more demanding than static imaging applications.

## Conclusion

This brings us back to the beginning of this lecture and the subject of perspectives. A saying attributed to Buddha is “The way is not in the sky. The way is in the heart.” I believe that for nuclear medicine and molecular imaging the way may be partially in the sky, but part is also certainly in the heart. Perspectives that we gleaned from this meeting indicate some aspects of the directions in which this will take us in the future. Cardiovascular imaging will play lead roles in clinical implementation of absolute quantification, in solid-state detector SPECT, and in comprehensive, pathway-driven implementation of molecular imaging (in inflammation, infarct, and plaque).

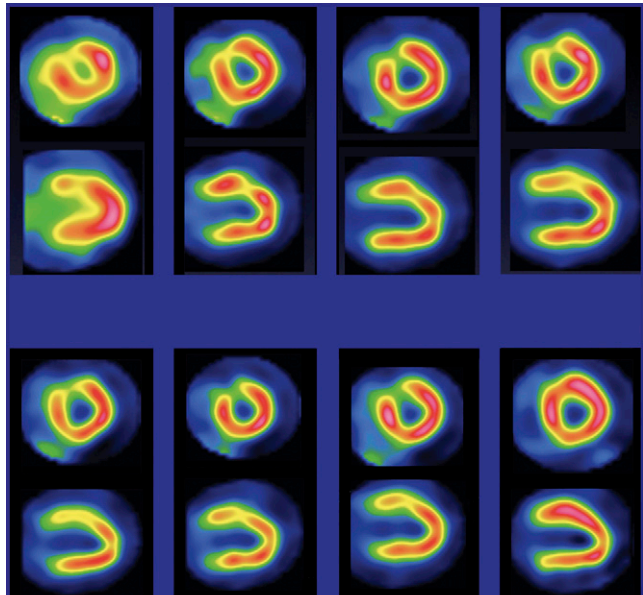


**FIGURE 17.** Dual-isotope SPECT with dynamic acquisition using a fast gamma camera with a CZT detector in a 69-y-old man with hypertrophic cardiomyopathy. Top 2 rows: Dynamic SPECT data acquired at (left to right) 2–5, 5–8, 8–11, and 11–14 min after  $^{123}\text{I}$ -BMIPP injection. Bottom 2 rows: Left 2 columns: continued serial images acquired at 14–17 and 17–20 min after  $^{123}\text{I}$ -BMIPP injection. Right 2 cols: Early  $^{123}\text{I}$ -BMIPP images and  $^{99\text{m}}\text{Tc}$  tetrofosmin images.

On my personal wish list for next year, at the SNMMI 2013 Annual Meeting, I would like to see more focus on multimodality integrative imaging. I would also like to see more first-in-human studies that tackle the translational challenges of advancing current preclinical studies to beneficial applications. And I would like to see more researchers thinking (and acting) beyond traditional organ boundaries to focus on the mechanisms (such as cell trafficking, immune signaling, and metabolism) that play a role not only in the cardiovascular system but in a variety of other systems and diseases as well.

Frank M. Bengel, MD  
Hannover Medical School, Germany

## Neurosciences Highlights

The society now has a new name—the Society of Nuclear Medicine and Molecular Imaging (SNMMI)—and is looking to the future. At the same time, I want to honor Henry N. Wagner, Jr., MD, who for many years gave the annual Highlights Lecture at this meeting. I had the pleasure of seeing him earlier this year in Hamamatsu, Japan. He remains enthusiastic about advances in neurologic molecular imaging. As you may know, he put himself into a scanner in 1983 at Johns Hopkins for the first *in vivo* *in-human* molecular imaging of brain dopamine receptors by PET (*Science* 1983;221:1284–1266). After 30 y we have a growing number of radiotracers available in the United States for research and clinical studies (e.g., perfusion SPECT, <sup>18</sup>F-FDG PET, amyloid PET, dopamine SPECT), which reflects remarkable accomplishment and a tremendous amount of effort. Many of the studies on this exciting journey have been presented at SNM meetings.

### Imaging Dementia

At this meeting, because of the new approval of a radiotracer for amyloid imaging and the growing importance of dementing disorders in our society, many papers focused on dementia imaging. The technical translation from initial basic science to human applications is a long and difficult effort, including strict requirements for validation that the tracer actually works as intended in humans. Wong et al. from Johns Hopkins University (Baltimore, MD), the University of Turku (Finland), the University of Pennsylvania (Philadelphia), Kuopio University Hospital (Finland), and GE Healthcare (Princeton, NJ) reported on “Association between <sup>18</sup>F-flutemetamol PET imaging and amyloid deposition in cortical brain biopsies from normal pressure hydrocephalus [NPH] subjects” [147]. They found that <sup>18</sup>F-flutemetamol uptake demonstrated strong concordance with *in vivo* amyloid- $\beta$  biopsy in patients with NPH (Fig. 1), regardless of timing and sequence of examinations, and shows promise as an imaging tool for detection of amyloid- $\beta$  both in patients with suspected NPH and possibly in the wider population.

Another multicenter trial on a different new PET amyloid tracer was that of Sabri et al. from the University of Leipzig (Germany), Choju Medical Institute (Fukushima, Japan), Hamamatsu Medical Center (Japan), Koseikai Hospital (Japan), Tokyo Metropolitan Geriatric Hospital (Japan), Georg-August University (Göttingen, Germany), Bayer Healthcare (Berlin, Germany), and Banner Health (Sun City, AZ), who reported on a “Multicenter phase 3 trial on florbetaben for  $\beta$ -amyloid brain PET in Alzheimer disease [AD]” [41]. Their research showed very close correlation between imaging and autopsy data (Fig. 2).

One exciting part of new tracer development is that with the advent of widespread and varied preclinical imaging instrumentation, we can test these tracers in small animals, even longitudinally, and at the end of the study compare serial imaging results with autoradiographic data from the same animals. One example of such a study was that of Rominger et al. from the University of Munich (Germany) and Hoffman-La Roche (Basel, Switzerland), who reported on “Longitudinal assessment of cerebral amyloid- $\beta$  deposition in APP-Swe mice with <sup>18</sup>F-florbetaben PET” [92] (Fig. 3).

Many groups are researching new and improved amyloid tracers for PET imaging. Rowe et al. from Austin Health, the

Mental Health Research Institute, and the University of Melbourne (all in Melbourne, Australia) and AstraZeneca R&D (Södertälje, Sweden) reported on “Comparison of <sup>11</sup>C-PiB and <sup>18</sup>F-AZD4694 for A $\beta$  imaging in aging and dementia” [149]. Their study showed that with the same acquisition timing, processing, and display scale the new tracer closely replicated the detail achieved with <sup>11</sup>C-PiB imaging (Fig. 4). The advantage of an <sup>18</sup>F-labeled tracer for these applications would be easier distribution throughout the country. It is to be seen whether this tracer will become clinically available.

Because amyloid imaging has already been performed for several years, we are seeing increasing numbers of informative studies with longitudinal data. Ong et al. from Austin Hospital, The Mental Health Research Institute, and the University of



**Satoshi Minoshima,  
MD, PhD**

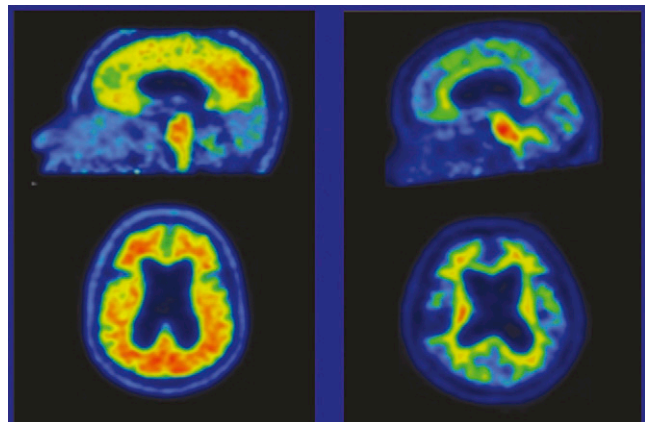


**FIGURE 1.** <sup>18</sup>F-flutemetamol PET was positive in patients with normal pressure hydrocephalus (left) and negative in healthy subjects (right).

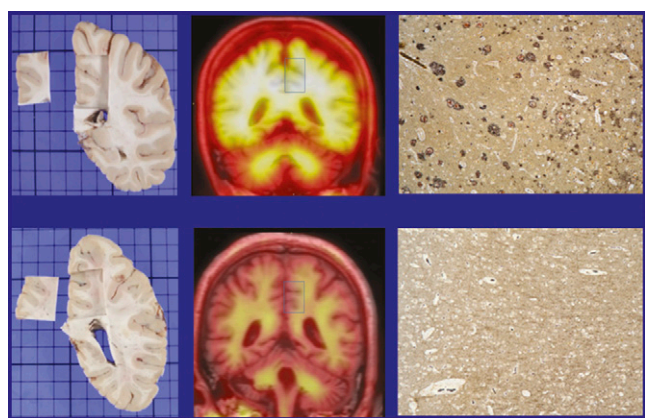


**FIGURE 2.** <sup>18</sup>F-florbetaben PET and histopathology in (top) AD patient, where amyloid-positive images correlated well with histopathology (note gray/black deposits, right); and (bottom) subject without AD, where absence of tracer uptake correlated with absence of amyloid deposits in histopathology.

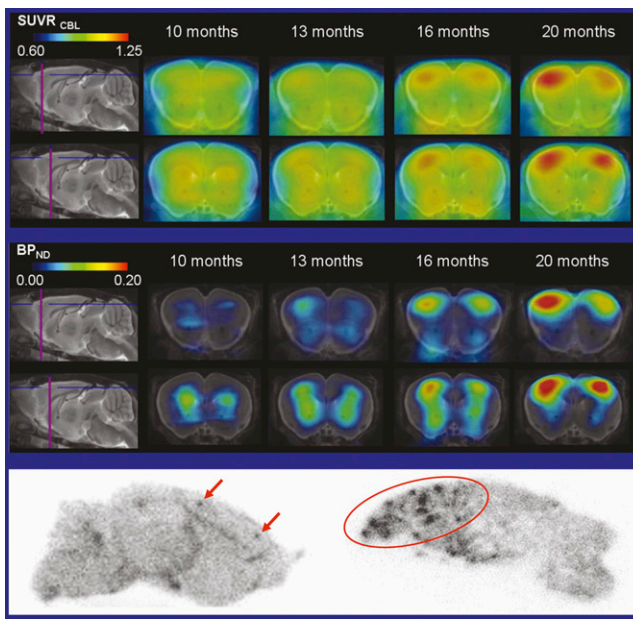


**FIGURE 3.** Serial <sup>18</sup>F-florbetaben PET assessment (at 10–20 mo) of cerebral amyloid deposition in a mouse model of AD. Top: Parametric binding potential images. Middle: Standardized uptake value ratio images. Bottom: Ex vivo autoradiography showing (left) slight amyloidosis at 13 mo and (right) distinct amyloidosis at 20 mo.

Melbourne (all in Melbourne, Australia) and Bayer Pharma AG (Berlin, Germany) reported on “Two-year longitudinal assessment of A $\beta$  deposits in mild cognitive impairment [MCI] with <sup>18</sup>F-florbetaben” [148]. They found that simple visual assessment of <sup>18</sup>F-florbetaben PET images as normal or abnormal successfully predicted which patients with MCI would progress to AD over the

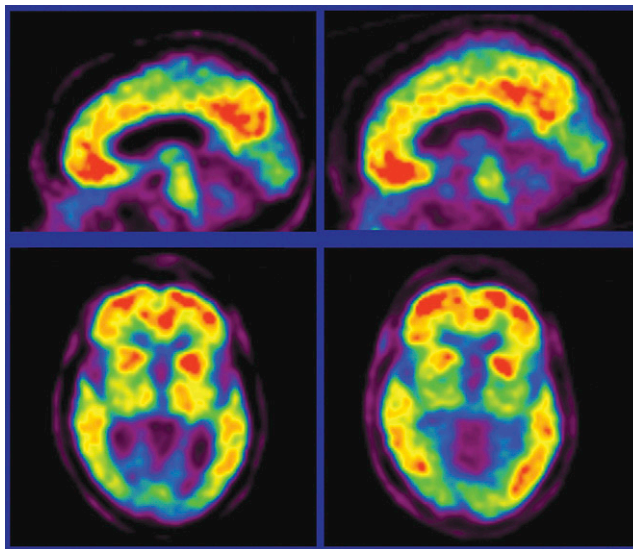


**FIGURE 4.** Results in PET imaging in an individual with AD were similar with the novel tracer <sup>18</sup>F-AZD4694 (left) and <sup>11</sup>C-PiB using the same acquisition timing, processing, and display scale.

24-mo follow-up period (Fig. 5). These and other data suggest that this tracer could serve as a remarkable biomarker to predict disease progression.

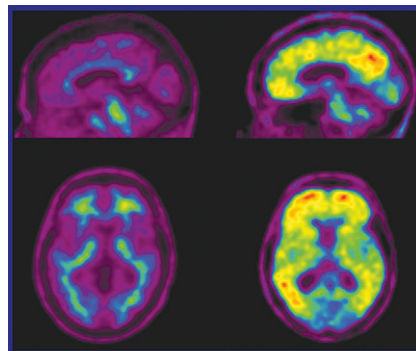
Similar findings were identified by Rowe and many of the same researchers from Austin Health, The Mental Health Research Institute, the National Ageing Research Institute, and the University of Melbourne (all in Melbourne, Australia), Edith Cowan University (Perth, Australia), and the Australian e-Health Research Centre (Brisbane), who reported on “Imaging and cognitive biomarkers as predictors of progression to AD” [299]. This group, part of the Australian Imaging Biomarkers and Lifestyle Flagship Study of Ageing, followed patients and control subjects for 3 y. Among their findings was the fact that healthy controls whose initial amyloid imaging was positive were much more likely to develop MCI or AD over the 3-y study period. This indicates that amyloid imaging can predict future onset of disease in asymptomatic individuals.

These predictive powers were also studied by Joshi et al. from Avid Radiopharmaceuticals for the AV-45 A11 investigators, who reported on “Use of florbetapir-PET to assess progression of amyloid burden over time” [89]. Repeat images clearly showed progressive amyloid accumulation in those patients who were deemed by the initial scan as likely to develop MCI or AD.

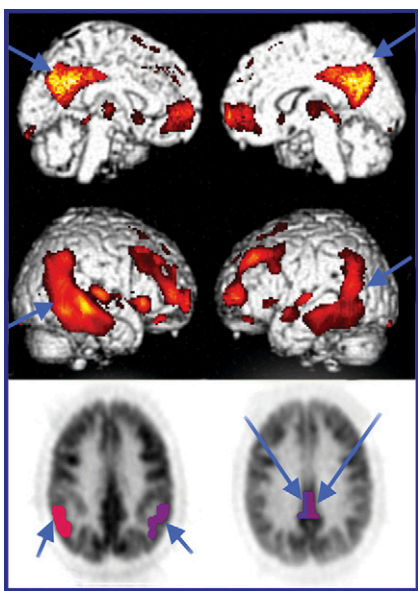
This kind of prediction was also the subject of a presentation by Torosyan et al. from the University of California, Los Angeles, who reported on the “Prognostic value of PET scans for predicting rate of functional decline of normal and MCI subjects over 3 y” [301]. Their images nicely showed that the degree of hypometabolism can predict the rate of cognitive decline (Fig. 6). They presented a dementia–prognosis index that can predict the rate of functional decline in the years following baseline PET.

Image analysis assumes a key role in these studies. Different methods can produce different findings. Standardizing some of these imaging analysis techniques will become a major focus in neuroscience in the near future. This was emphasized by the findings of Su et al. from Washington University School of Medicine (St. Louis, MO), who reported on “Patterns of amyloid deposition and glucose metabolism in autosomal dominant AD: comparison of quantification methods” [88].

This is an exciting time, when molecular imaging is entering the clinic. Ossenkoppele from VU Medical Center (Amsterdam, The Netherlands) described the “Diagnostic value of molecular imaging in a memory clinic setting” [303]. These researchers looked at the specific ways in which molecular imaging benefited patients. They found that FDG and/or PiB imaging were most



**FIGURE 5.** Simple visual assessment of <sup>18</sup>F-florbetaben PET predicted which patients with MCI would (right) and would not (left) progress to AD over a 2-y period.



Bottom images show automatically determined subvolumes of interest. Colors indicate voxels where baseline metabolism correlated significantly with subsequent functional decline.

helpful in those patients in whom diagnoses were uncertain. When neurologic molecular imaging becomes well integrated into clinical routines, such patients will benefit.

One important part of acceptance for these techniques rests on the ability of the nuclear medicine physician to supply accurate interpretation of data. This is still challenging, in part because advanced and continuously evolving technologies can produce confusing images. This topic was addressed by Xu et al. from the University of Wisconsin School of Medicine and Public Health (Madison), who reported on "Visual assessment of  $^{11}\text{C}$ -PiB PET and  $^{18}\text{F}$ -FDG PET for detection of amyloid burden and abnormal metabolism among cognitively normal middle-aged adults with high risks for AD" [91] (Fig. 7).

Image analysis techniques can enhance confidence in image interpretation. An example was that presented by Frey et al. from

the University of Michigan (Ann Arbor) and the University of Washington (Seattle), who reported that "Surface projection maps of cortical amyloid binding reveal canonical patterns in neurodegenerative dementias" [144]. This is a standardized way to present amyloid imaging in individual cases for diagnostic purposes. In Figure 8 amyloid imaging clearly distinguishes dementia with Lewy bodies (DLB) from frontotemporal dementia, a distinction that can be clinically difficult. Image analysis technology can improve advanced imaging and its acceptance. SNMMI and industry are currently working to provide teaching materials on new tracers and relevant interpretation and analysis techniques, and these will be available online.

When new molecular imaging technologies become available, they are also applied to basic science research questions. Ossenkoppele et al. from the VU Medical Center (Amsterdam, The Netherlands) reported on "Increased parietal amyloid burden and metabolic dysfunction in AD with early onset" [90]. This presentation won the first-place Brain Imaging Council Young Investigator Award. The group looked at different types of AD patients, some of whom developed dementia before the age of 65 y and many more of whom developed dementia at older ages. The clinical profiles of these 2 groups are clearly different. Participants underwent both  $^{18}\text{F}$ -FDG and  $^{11}\text{C}$ -PiB scans, and differences in regional uptake were assessed. The researchers found that the younger group had greater glucose metabolic reduction and more amyloid deposition in the parietal lobe. These findings were correlated with cognitive decline profiles, with the conclusion that the clinical difference between younger and older AD patients may be related not only to topographic differentiation in downstream processes but may originate from distinctive distributions of early upstream events.

A unique study was presented by Klupp et al. from the Technische Universität Munich (Germany), who reported that "In AD, hypometabolism in brain regions less affected by amyloid pathology may be a consequence of pathologies in functionally connected brain regions" [305]. They looked at the complicated brain networks responsible for cognitive decline in AD. When FDG and amyloid scans are performed in the same patient we often see a discordance in terms of spatial distribution of hypometabolism and amyloid deposition. This group looked at those areas that did not have high amyloid deposition but did show hypometabolism.

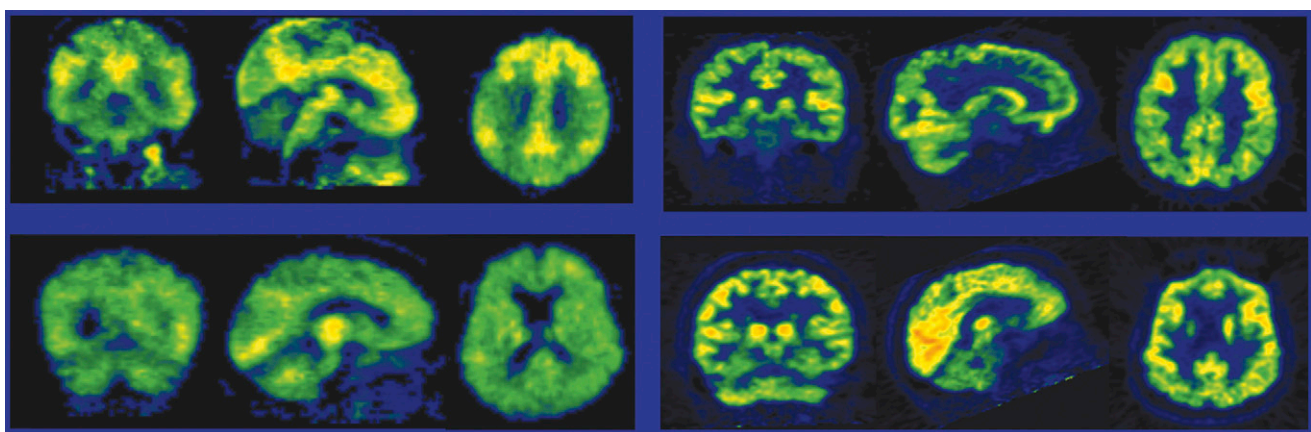
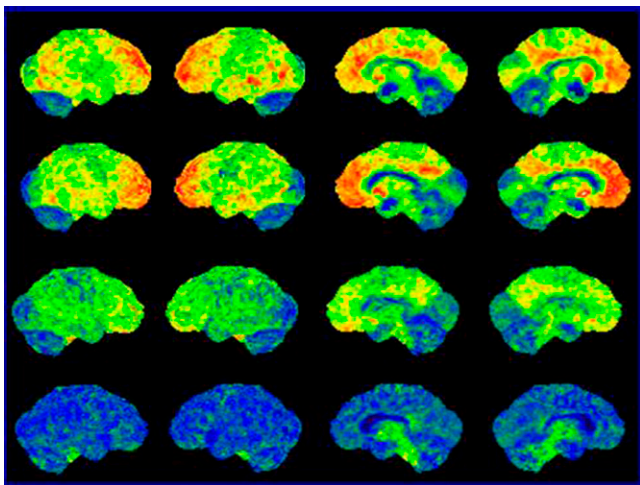


FIGURE 7. Comparison of  $^{11}\text{C}$ -PiB and  $^{18}\text{F}$ -FDG PET images in cognitively normal individuals with high risk for AD. Top: Subject with AD-positive pattern of  $^{11}\text{C}$ -PiB uptake (left) and AD-possible pattern of  $^{18}\text{F}$ -FDG uptake (right). Bottom: Different subject with AD-positive pattern of  $^{11}\text{C}$ -PiB uptake (left) and normal pattern of  $^{18}\text{F}$ -FDG uptake.



**FIGURE 8.** Amyloid binding maps derived from single-subject imaging clearly differentiate among different disease patterns. Subjects with: (top row) AD, (second row) PD, (third row) DBL, and (fourth row) frontotemporal dementia.

They also used resting-state MR imaging to look at the brain network system and discovered that some of the areas without much amyloid deposition have profound hypometabolism (Fig. 9). Those areas tend to be functionally connected with brain regions most damaged by amyloid. These results support the idea that hypometabolism in brain regions not strongly affected by amyloid pathology may be caused by diminished neuronal input from affected regions. Behind the clinical images we typically see, then, very complex brain networks are affected differentially by AD processes.

Expanding on these network concepts, Yakushev et al. from the Technische Universität Munich (Germany), University Medical Center Mainz (Germany), Inserm-EPHE-Université de Caen (France), and the University of Liège (Belgium) reported that “Metabolic and structural connectivity within the default mode network relates to working memory in young healthy adults” [304]. They looked at both FDG scan results and functional MR analysis of brain networks using a diffusion tensor imaging tractography pulse sequence (Fig. 10). Tract density in the cingulate bundle connecting the medial prefrontal cortex and the posterior cingulate cortex correlated with FDG uptake in the same area, one that is associated with verbal working memory and is severely impaired in AD patients. With an understanding of the pathophysiology behind molecular imaging results, it is clear that the brain

**FIGURE 9.** Areas without much amyloid but with profound hypometabolism are functionally connected to brain regions most damaged by amyloid. White = seed; blue = overlap between hypometabolism and amyloid pathology; red = connecting areas; and fuschia = overlap of blue and red areas.

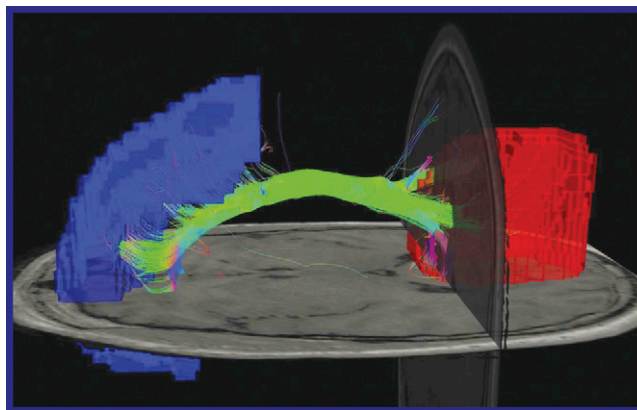
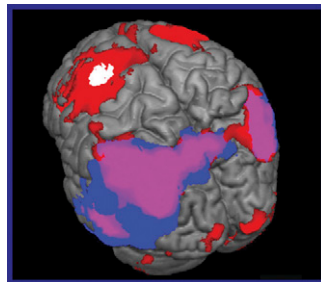


**FIGURE 10.** Diffusion tensor imaging from default mode network hubs. Blue = medial prefrontal cortex; green = cingulate bundle; and red = posterior cingulate cortex. Tract density in the cingulate bundle correlated with FDG uptake.

works as an integrated network. Some parts of this network are severely affected in AD, resulting in abnormal FDG metabolism and in clinical symptoms.

All of these diagnostic efforts can be optimally applied to patient care only when we have effective treatments to apply in AD. Many researchers are using molecular imaging to advance understanding of the ways in which therapeutic drugs can work in AD patients. Brownell et al. from the Massachusetts General Hospital, Harvard Medical School, and the VA Boston Healthcare System (all in Boston, MA) used a transgenic AD model in their study “Ibuprofen reduces inflammatory response in Alzheimer mice” [415]. One interesting observation made over the last 20 y is that the Alzheimer-affected brain has significant activated neuroinflammation that can be detected with molecular imaging, in this case an  $^{11}\text{C}$ -labeled tracer. When transgenic mice mimicking AD were treated with an anti-inflammatory drug (ibuprofen) the reduction of inflammatory activity was clearly visible (Fig. 11). These types of methodologic approaches

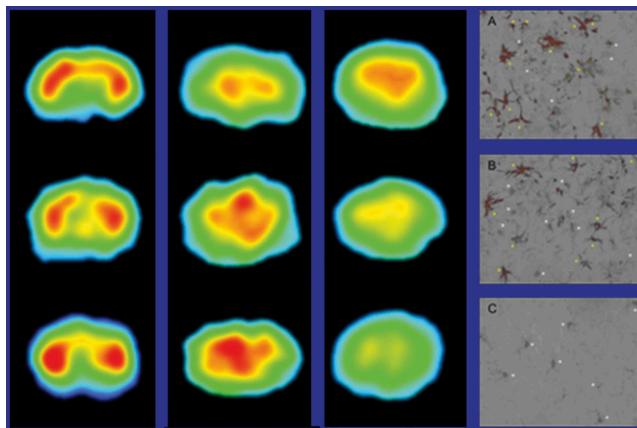


**FIGURE 11.** Ibuprofen-induced modulation of mGluR5 in AD mice imaged with  $^{18}\text{F}$ -FPEB (left column), glucose utilization with  $^{18}\text{F}$ -FDG (second column), inflammatory response with  $^{11}\text{C}$ -PK11195 (third column), and ex vivo stained microglia (right column). Experimental groups included (top row) 3xTg-AD mice; (middle row) 3xTg-AD mice treated with ibuprofen; and (bottom row) controls.

and proof-of-concept studies can advance therapeutic development in AD.

## Neuroinflammation and Cholinergic Investigations

Neuroinflammation is not specific to AD, and many people are finding that it plays a role in a range of neurologic disorders. One example was the presentation by Ribeiro et al. from Université François Rabelais (Tours, France) and the University of Sydney (Australia), who reported on “Evaluation of neuroinflammation in amyotrophic lateral sclerosis [ALS] with  $^{18}\text{F}$ -DPA-714” [35]. Patients with ALS had slightly elevated neuroinflammation when compared with normal controls (Fig. 12).

Many researchers are developing better tracers to visualize neuroinflammation. Zepper et al. from McGill University (Toronto, Canada) and Imperial College (London, UK) reported on “Evaluation of a new  $^{18}\text{F}$  radiotracer (PBR06) for microglia imaging in stroke” [93].

Acetylcholine (cholinergic) investigation is important in AD as well. The U.S. Food and Drug Administration has approved symptomatic therapeutics for AD, and the majority of these are cholinergic modulators. Meyer et al. from the University of Leipzig (Germany) reported on “Differentially decreased  $\alpha 4\beta 2^*$ -nicotinic receptor ( $\alpha 4\beta 2^*$ -nAChR) availability in early-onset (EOAD) and late-onset AD” [39]. They found that cholinergic abnormality was much more severe in the EOAD group and correlated with severity of symptoms (Fig. 13).

Because of continued interest in this area, new drugs are being developed to image the cholinergic system in the human brain. Hillmer et al. from the University of Wisconsin (Madison) and the University of California, Irvine reported on “Quantitative analysis

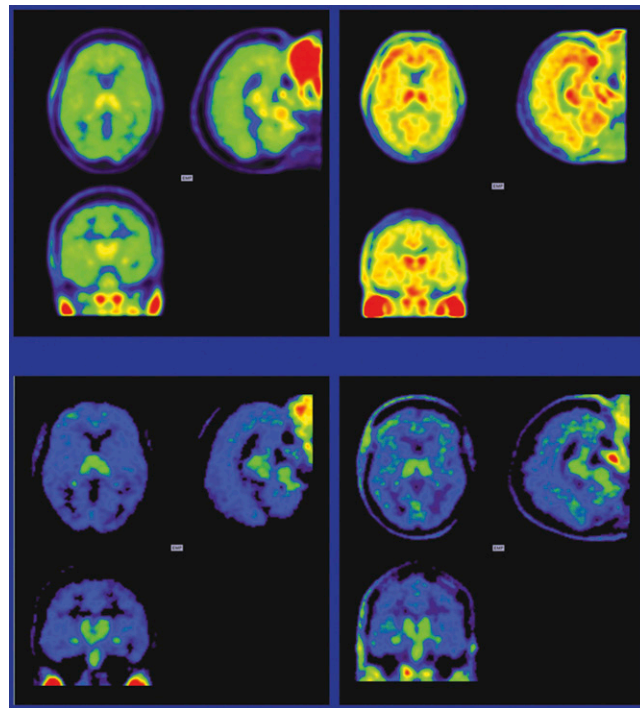


**FIGURE 12.** Neuroinflammation imaging in (left) controls and (right) ALS patients shows (top)  $^{18}\text{F}$ -DPA-714 integrated images and (bottom)  $^{18}\text{F}$ -DPA-714 distribution volume relative images.

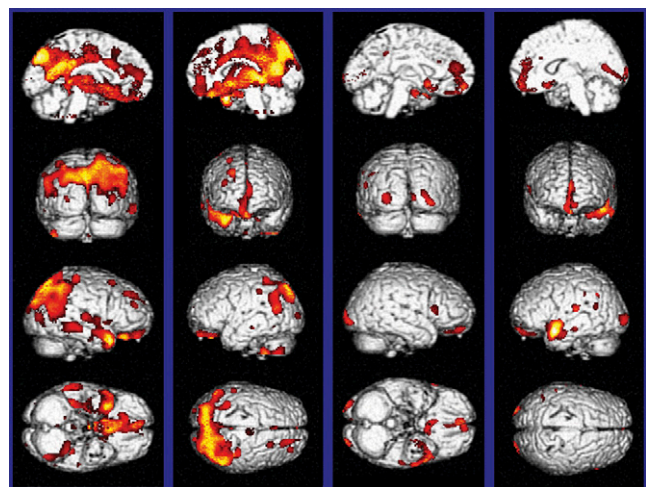


**FIGURE 13.** Reduced  $\alpha 4\beta 2^*$ -nAChR binding in early (left 2 columns) and late (right 2 columns) -onset AD with  $2-^{18}\text{F}$ -F-A85380 (2FA) PET.

of  $^{18}\text{F}$ -nifene kinetics in the nonhuman primate” [94]. The presentation won the second-place Brain Imaging Council Young Investigator Award. Figure 14 nicely shows cholinergic uptake and blocking with this tracer.

Other groups are using more advanced approaches. Esterlis et al. from Yale University (New Haven, CT) reported on “Imaging acetylcholine effects on  $^{123}\text{I}$ -5-IA-85380 binding to  $\beta 2$ -nicotinic acetylcholine receptors: physostigmine studies in human subjects” [411]. These researchers were able to perform blocking studies to infer the amount of acetylcholine concentration in the synaptic cleft. Thus molecular imaging can look beyond receptors to potentially elucidate how much acetylcholine is available in the synaptic cleft for modulation of brain function. This kind of technology is becoming more widely available in the neuroscience field.

A unique study from Mukhin et al. from the Duke University Medical Center (Durham, NC) and the Wake Forest University Baptist Medical Center (Winston-Salem, NC) described “Prediction of brain nicotine accumulation during cigarette smoking using data obtained after a single puff of  $^{11}\text{C}$ -nicotine-containing cigarettes” [200]. The radiolabeled nicotine was incorporated into a cigarette, with brain imaging following inhalation of a single puff. Although tobacco smoking is characterized by intermittent

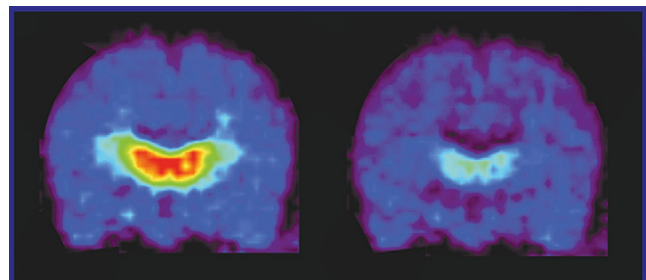


**FIGURE 14.** Two-injection  $^{18}\text{F}$ -nifene study in baboon. Summed postinjection images normalized to the same scale. Left: High-specific-activity  $^{18}\text{F}$ -nifene uptake at 20–40 min postinjection. Right: Dramatically decreased tracer uptake as a result of injection of 18 nmol cold nifene at 60 min.

puffing, the researchers found that nicotine uptake in the brain is much more continuous, gradually rising, with some delay from the start of smoking to maximum transfer of nicotine to the blood and cerebrospinal fluid. These types of pharmacokinetic studies help us to better understand how nicotine from cigarettes affects human brain function.

The nicotinic system is not unique to AD and can be impaired in Parkinson disease (PD) as well. Bohnen et al. from the University of Michigan (Ann Arbor) reported on "Heterogeneity of cholinergic denervation in PD" [470]. This team looked at the differential involvement of cholinergic systems in PD. They investigated cortical and thalamic acetylcholinesterase activity using  $^{11}\text{C}$ -PMP PET in patients with PD and compared these with normal values in non-PD control subjects. They found that cortical acetylcholinesterase loss was associated with cognitive impairment independent from loss of dopamine. Thalamic (pedunculopontine nucleus) acetylcholinesterase loss was associated with a history of falls and rapid eye movement sleep behavior disorder. They concluded that cholinergic denervation in PD without dementia is heterogeneous, with corresponding clinical phenotypic variation.

Dopamine transporter (DAT) imaging is available for PD imaging, and we know that dopamine is a central neurochemical system affected in PD. But other neurochemical systems are involved in PD, and understanding these can potentially explain some of the nonmotor abnormalities associated with the disease. Varrone et al. from the Karolinska Institutet (Stockholm, Sweden) and Stockholm University (Sweden) reported on "5-HT<sub>1B</sub> receptor imaging in PD with  $^{11}\text{C}$ -AZ10419369 and PET" [472]. They used this serotonin ligand tracer to show a major decrease of serotonin binding potential in limbic regions and temporal cortex in patients with PD (Fig. 15).

Other neurochemical systems can be imaged in PD. Brownell et al. from the Massachusetts General Hospital and Harvard Medical School (Boston, MA) and the McLean Hospital (Belmont, MA) reported on "Modulation of metabotropic glutamate subtype 5 receptor (mGluR5) in dyskinesia" [468]. Figure 16 shows initial results in nonhuman primates in which experimental dopamine reduction mimicked PD and dyskinesia. Cortical glutamatergic uptake increased after the monkeys developed PD or dyskinetic symptoms. This kind of study is interesting because it shows the ways in which a new tracer can reveal interactions within the neurochemical systems, elucidate the complexity of brain mechanisms, and explore the interaction of disease processes with multiple neurochemical systems.

Ziebell et al. from the Rigshospitalet, Bispebjerg Hospital, Roskilde Hospital, and the University of Copenhagen (all in Denmark) reported that "Striatal DAT binding in patients with DLB is not associated with clinical severity" [471]. The dopamine system is also impaired in DLB, but this impairment was not found to correlate with hallucinations or fluctuations in disease. Other mechanisms must be at work, then, in some of the critical symptoms that we see in some patients with dementia.

## Complex Connections

Dr. Wagner often highlighted in his lectures the importance of combining molecular imaging, genetics, and pharmacology to provide tools that will allow us to better understand neuroscience and also revolutionize medical practice. Today his vision is becoming a reality.

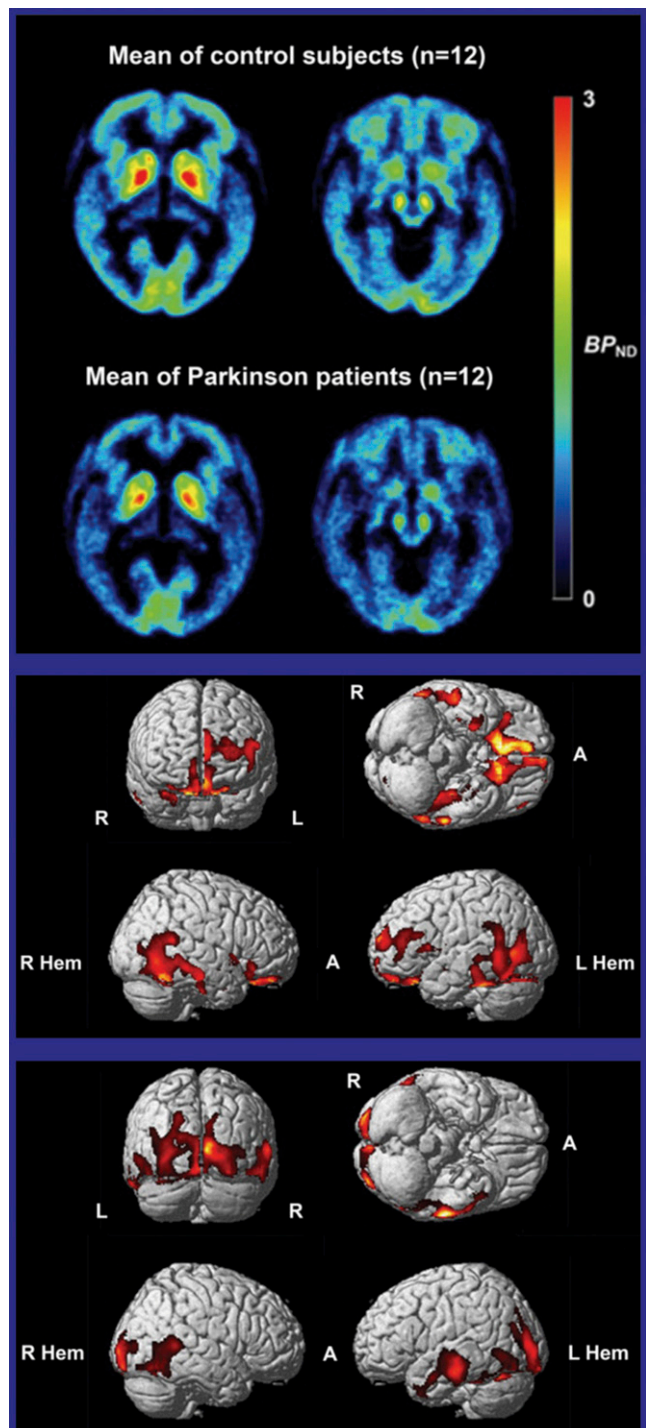


**FIGURE 15.** 5-HT<sub>1B</sub> receptor availability imaging with  $^{11}\text{C}$ -AZ10419369 PET. Top block: PET images in (top) controls and (bottom) patients with PD. Voxel-based analyses showed trend toward global decrease in binding potential in PD, with (middle block) significant decreases in limbic regions and temporal cortex and (bottom block) significant negative correlation between disease duration and 5-HT<sub>1B</sub> receptor availability in primary and associative visual cortex.

Bonab et al. from the Massachusetts General Hospital and Shriners Hospital Boston (both in Boston, MA) reported on "Effects of DATgene polymorphisms and attention deficit hyper-

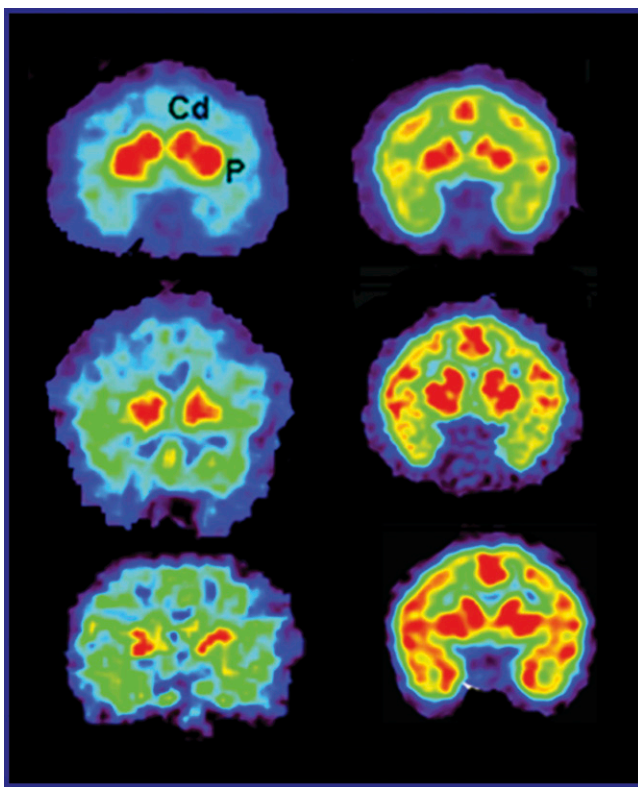


**FIGURE 16.** Imaging of modulation of dopamine transporter (left, with  $^{11}\text{C}$ -CFT) and mGluR5 (right, with  $^{18}\text{F}$ -FPEB) function in (top) control, (middle) parkinsonian syndrome, and (bottom) dyskinesia in *macaca fascicularis*.

activity disorder [ADHD] status on DAT binding measured with PET” [2013]. The group looked at the relationship between central DAT activity in the striatum in individuals with and without ADHD, with special attention to polymorphisms of the *DAT1* (*SLC6A3*) gene (3'UTR and intron 8 VNTR). They hypothesized that there would be a significant association between these DAT gene polymorphisms (and haplotype) and DAT binding activity in the striatum in individuals with ADHD. Instead, they found that only the 3'UTR polymorphism was associated with impaired DAT binding in both ADHD and healthy controls. They also found that both ADHD status and 3'UTR polymorphism status had an additive effect on DAT binding. This suggested that an ADHD risk polymorphism (3'UTR) has functional consequences on central nervous system DAT binding in humans.

Shumay et al. from the Brookhaven National Laboratory (Upton, NY) and the National Institute on Drug Abuse (NIDA; Bethesda, MD) reported on “Exploring the links between the brain DAT availability, *DAT1* genotype, and body mass index [BMI]” [195]. They looked at the 9R/9R genotype, in which lower DAT availability and higher BMI were found to be correlated (Fig. 17). They concluded that by modulating DAT expression, the *SLC6A3* genotype can affect an individual’s sensitivity to food-associated reward. So the dopaminergic system, which is important in AD, PD, DLB, and other diseases is also a potential target for modulating weight.

A recent media report indicated that sleep deprivation today in the United States is most often the result of professional stress and that such deprivation is associated with a 4-fold risk of stroke. One

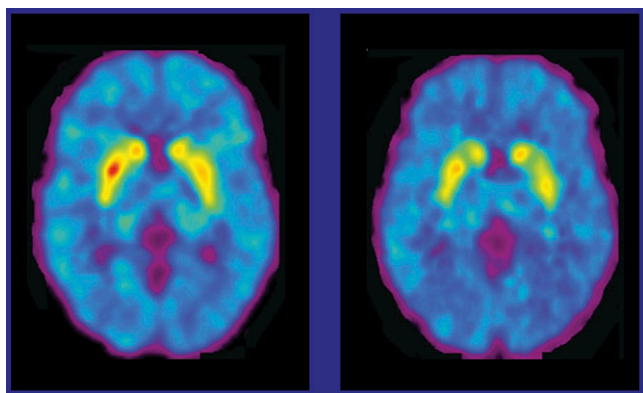


**FIGURE 17.** Striatal DAT images in individuals with the 9R/9R genotype. Left: Age 39 y old; BMI = 23 kg/m<sup>2</sup>. Right: Age 37 y old; BMI = 31 kg/m<sup>2</sup>.

group looking at the reasons behind the negative effects of sleep deprivation is that of Volkow et al. from NIDA (Bethesda, MD) and Brookhaven National Laboratory (Upton, NY), who reported that “Sleep deprivation decreases striatal D2R availability without increasing dopamine release” [196]. They discovered that dopamine receptor availability is decreased in sleep-deprived conditions (Fig. 18). This decrease is not the result of increased intrasynaptic dopamine release, because a drug challenge study did not show any changes expected with such a release. The pathophysiology of sleep deprivation and the role of dopamine will be the focus of more investigations using molecular imaging.

Dopamine is, of course, fundamentally related to human behavior. Vernaleken et al. from the Universitätklinikum Aachen (Germany) reported on “The impact of dopamine on behavior during an aggression provocation paradigm: an  $^{18}\text{F}$ -FDOPA PET study” [198]. Contrary to their expectation, they found an inverse correlation between tracer uptake and level of aggression (Fig. 19).

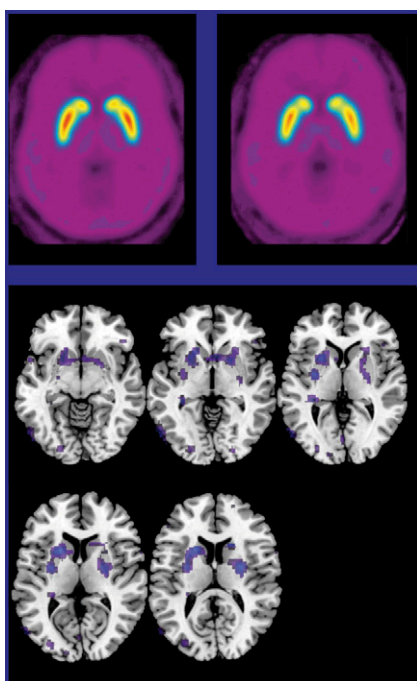


**FIGURE 18.** D2R binding assessed with  $^{11}\text{C}$ -raclopride PET in (top left) rested and (top right) sleep-deprived individuals. Statistical parametric mapping (bottom) showed decreased specific binding of  $^{11}\text{C}$ -raclopride in sleep deprivation.

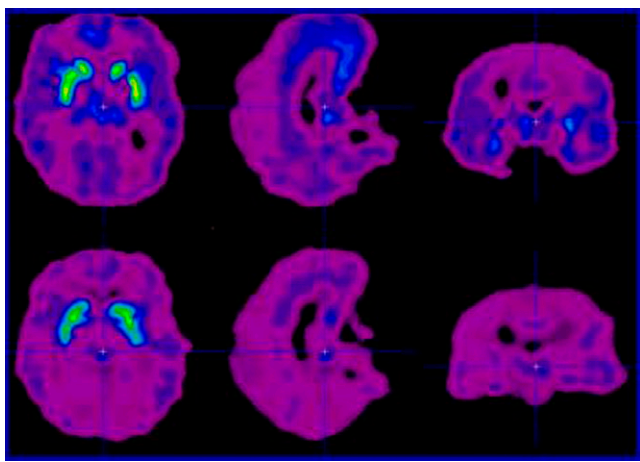


**FIGURE 19.**  $^{18}\text{F}$ -FDOPA uptake was found to correlate negatively with levels of aggression. Top row: low rates of aggression. Bottom row: high rates of aggression.

These are important studies and illustrate the fact that we have many miles to go in exploring the utility of molecular imaging technology in understanding human behavior.

SNMMI is an international society, and we have many submissions from the international community. The meeting provides an excellent opportunity for us to learn what is happening outside the United States. Yoon et al. from the Seoul National University Hospital (Seoul and Seongnag City, Korea) reported on the “Clinical utility of flumazenil [FMZ] PET vs. FDG PET and MR imaging in intractable epilepsy patients: prospective study with statistical parametric mapping method” [38]. They demonstrated that a combined approach using both tracers and both modalities can better diagnose epileptic seizure foci than a single modality. FMZ was also better able than FDG to detect neocortical abnormalities.

PET/MR imaging was also reported to be helpful in identifying epileptogenic foci. Maldonaldo et al. from the Hospital Ruber Internacional and Jesus Hospital (Madrid, Spain) reported on “PET-MRI in presurgical evaluation of refractory epilepsy associated with focal cortical dysplasia” [40]. Combining data from the 2 modalities achieved much higher accuracy, pinpointing for the neurosurgeon the appropriate areas for possible resection (Fig. 20). Many interesting sessions at this meeting included data

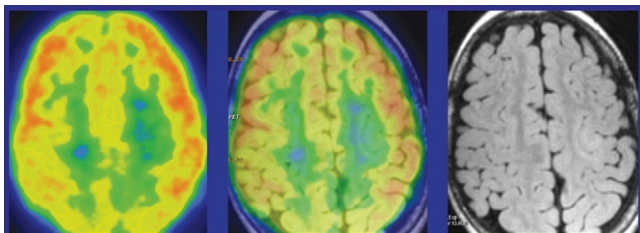


**FIGURE 20.** PET/MR imaging in patients with refractory epilepsy. Left:  $^{18}\text{F}$ -FDG PET detected metabolic changes in 80% of patients, including hypometabolism (90%), hypermetabolism (8%), and metabolic alterations in other regions with normal MR imaging in 27.5%. Right: 3T MR imaging showed findings suggesting focal cortical dysplasia (in this case in left frontal lobe, arrow) in 92%. Middle: PET/MR imaging detected lesions in 98% of patients.

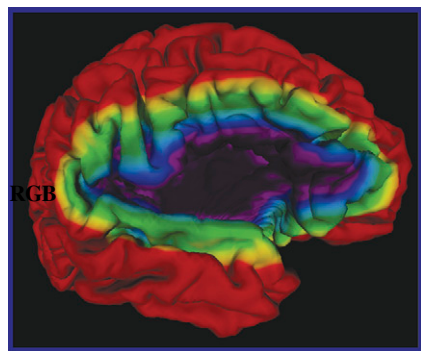


**FIGURE 21.** Delayed cell death imaging in subacute stroke using high-resolution  $^{18}\text{F}$ -flumazenil PET.

on integrated PET/MR imaging. Molecular imaging of epilepsy with these new scanners will undoubtedly be a focus of research and clinical applications.

Ischemic vascular research is still ongoing in nuclear medicine. Zepper et al. from Jewish General Hospital and McGill University (both in Toronto, Canada) and Ludwig Maximilian University (Munich, Germany) reported on “Imaging delayed cell death in subacute stroke with high-resolution  $^{18}\text{F}$ -FMZ” [37]. Cell death occurs at initial onset of stroke, but around the true core of the ischemic lesions are areas in which cells die more gradually. These researchers showed that these areas can be detected with  $^{18}\text{F}$ -FMZ, which is a central benzodiazapene system imaging agent (Fig. 21).

A unique tracer approach was presented by Kim et al. from Seoul National University Hospital (Korea) in their “Evaluation of neoangiogenesis after revascularization surgery in moyamoya disease using  $^{68}\text{Ga}$ -RGD PET/CT” [1954]. In patients imaged after surgery for moyamoya disease, the group showed that it is possible to visualize vessel revascularization (Fig. 22). These kinds of studies are revolutionizing our understanding of healing after ischemic or surgical events.

Application of molecular imaging in brain tumors is an important area of neurologic practice. In Europe,  $^{18}\text{F}$ -fluoroethyltyrosine is available. In Japan,  $^{11}\text{C}$ -methionine is available for clinical imaging. In the United States, unfortunately we are some-

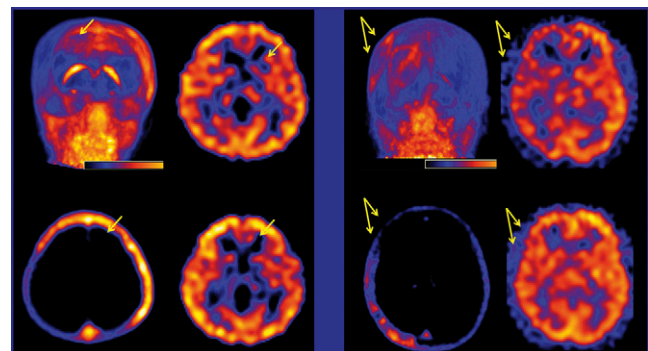


**FIGURE 22.**  $^{68}\text{GA}$ -RGD PET/CT in 2 patients after revascularization surgery in moyamoya disease. Left block: Patient with high tracer uptake shown in (left column)  $^{68}\text{GA}$ -RGD MIP (top) and transaxial (bottom) views and (right) after preoperative (top) and postoperative diamox administration (bottom). Arrows indicate mild-to-moderate vascular improvement. Right block: Patient with low tracer uptake shown in (left column)  $^{68}\text{GA}$ -RGD MIP (top) and transaxial (bottom) views and (right) after preoperative (top) and postoperative diamox administration (bottom). Arrows indicate good vascular improvement.

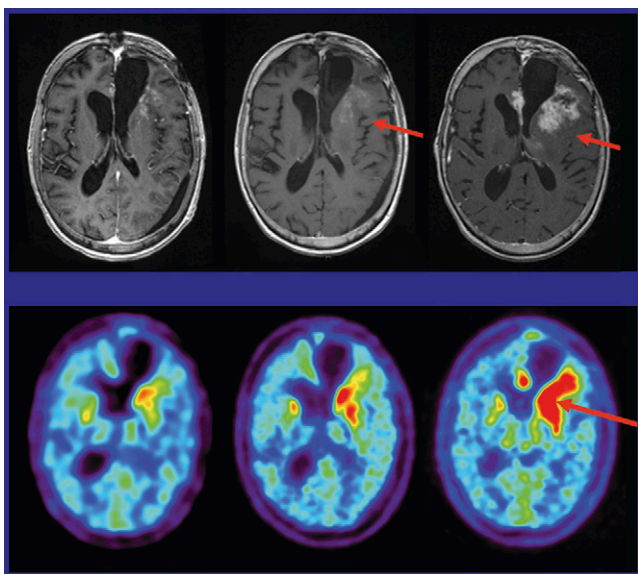


**FIGURE 23.** Imaging in patient with recurrent high-grade glioma. Top: MR images acquired at baseline and 6 and 12 wk after initiation of bevacizumab combination therapy. Tumor appeared stable at 6 wk but showed growth at 12 wk (arrows). Bottom:  $^{18}\text{F}$ -FDOPA PET images acquired at baseline and 1 and 2 wk after initiation of therapy showing tumor growth (arrow).  $^{18}\text{F}$ -FDOPA PET detected tumor growth as early as 9 d after start of therapy.

what behind in clinical use of new tracers.  $^{18}\text{F}$ -FDOPA is available on a limited scale. Schwarzenberg et al. from the University of California, Los Angeles, reported that “Metabolic tumor volume

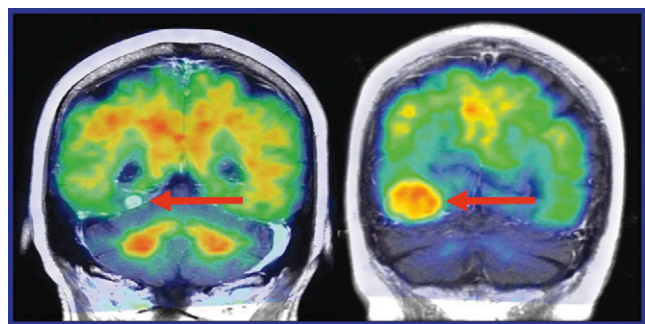


**FIGURE 24.** Coronal PiB PET/CT images fused with MR findings in patients with (left) melanoma metastasis and (right) meningioma. Both patients had tumors along the tentorium.

by  $^{18}\text{F}$ -FDOPA PET is predictive of treatment response in patients with recurrent high-grade gliomas as early as 2 wk after initiation of anti-angiogenic therapy” [250] (Fig. 23). They used this tracer to successfully predict therapeutic success and outcomes in patients with brain tumors.

Amyloid tracers, again, are becoming one of the most widely recognized molecular imaging technologies, both in research and more recently in the clinical setting, where new and exciting findings are being made. We think of amyloid imaging as specific to AD, but Johnson et al. from the Mayo Clinic (Rochester, MN) and the University of Pittsburgh (PA) reported on its use in meningiomas in their presentation “PiB PET/CT identification of meningiomas is not due to presence of amyloid- $\beta$  within tumors” [253]. Pathologic results from this study indicated that although the meningioma had amyloid tracer uptake, no amyloid deposition

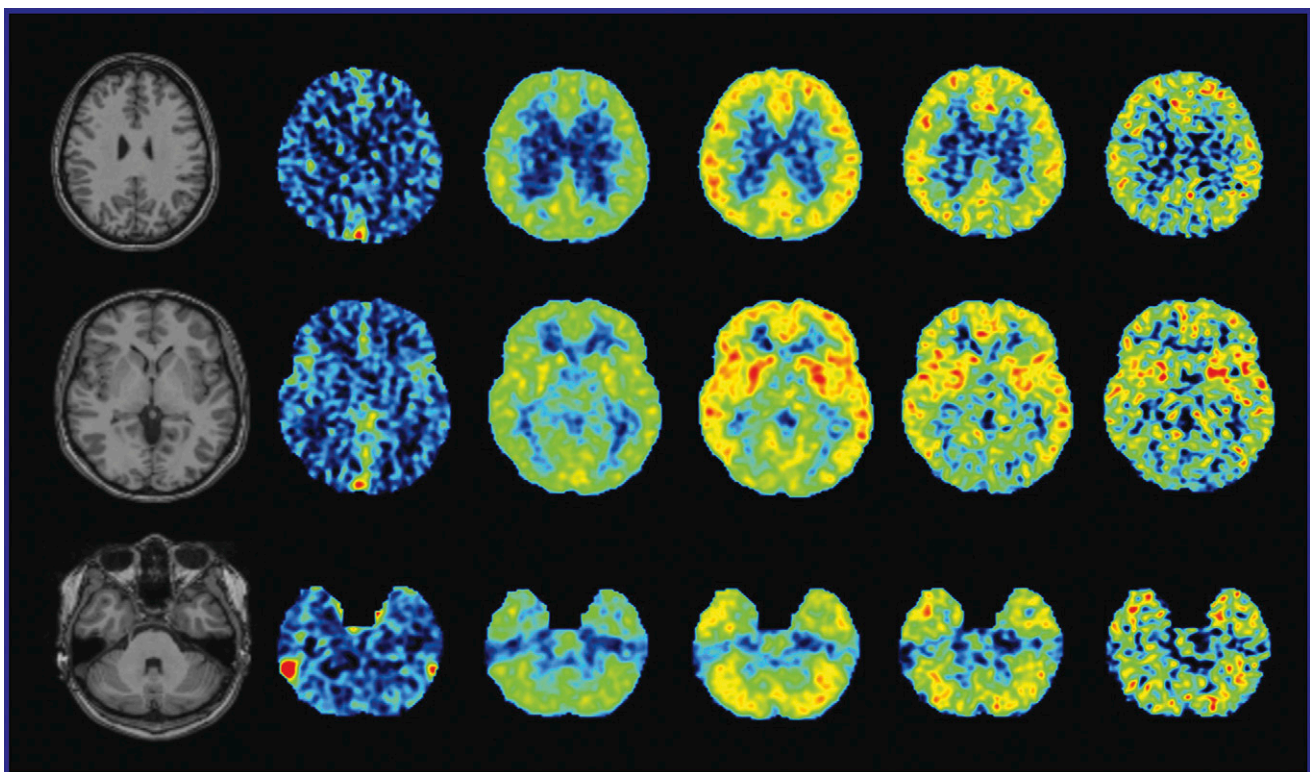


**FIGURE 25.**  $^{11}\text{C}$ -SD5024 and quantification of cannabinoid subtype-1 receptors in human brain. Left to right: MR images and  $^{11}\text{C}$ -SD5024 PET at 1, 7, 42, 77, and 112 min after injection.

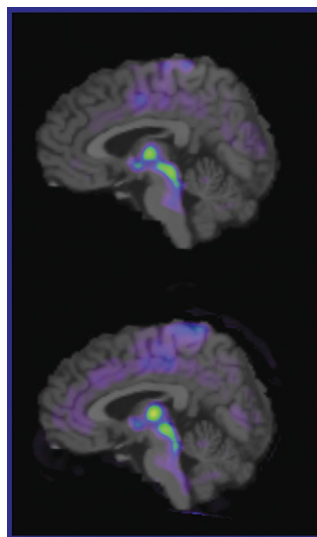


**FIGURE 26.** Mean parametric images from (top) healthy controls and (bottom) recently abstinent cocaine-addicted patients.

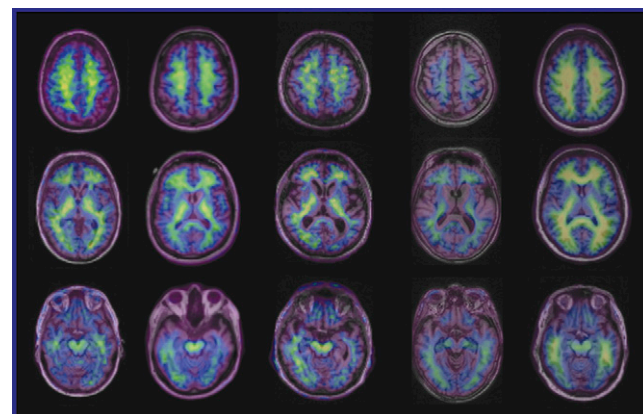


**FIGURE 27.**  $^{18}\text{F}$ -THK523 retention in PET imaging in different dementias. Left to right: healthy control ( $\text{A}\beta^-$ ); behavioral variant frontotemporal dementia ( $\text{A}\beta^-$ ); semantic dementia ( $\text{A}\beta^-$ ); progressive supranuclear palsy ( $\text{A}\beta^-$ ); and AD ( $\text{A}\beta^+$ ).

was present. We do not currently see this kind of case very often (Fig. 24), but once amyloid imaging and PET/MR are more common in the clinic, we may encounter more unexpected findings such as these.

## Multiple Pathways

The brain is complex, with numerous neurochemical substrates. One goal for neuroimaging is to identify and develop specific radiotracers that can be used to better understand this complex physiology and pathophysiology. Many such tracers are in the pipeline. For example, Prabhakaran et al. from Columbia University College of Physicians and Surgeons (New York, NY), Rigshospitalet and University of Copenhagen (Denmark), and New York State Psychiatric Institute (New York, NY) reported on “Evaluation of [ $^{11}\text{C}$ ]CIMBI-5 ([ $^{11}\text{C}$ ]IDME) as a 5-HT<sub>2A</sub> receptor agonist PET tracer in nonhuman primates” [1876]. Wong et al. from Johns Hopkins University (Baltimore, MD) and Hoffmann-La Roche (Basel, Switzerland) reported on “Imaging biomarkers for the glycine transporter type 1: human PET imaging of GlyT1 distribution and phase 1 drug occupancy” [199].

Tsujikawa et al. from the National Institute of Mental Health (Bethesda, MD) and the Karolinska Institutet (Stockholm, Sweden) reported on “Initial evaluation of [ $^{11}\text{C}$ ]SD5024, a novel PET radioligand for imaging human brain cannabinoid CB<sub>1</sub> receptors” [357]. They showed the kinetics of their tracer as it enters and is washed out of the brain (Fig. 25). This reversible ligand is well suited to PET imaging.

Lee et al. from Yale University (New Haven, CT) reported on “Imaging norepinephrine transporter in abstinent cocaine users using (S,S)-[ $^{11}\text{C}$ ]O-methylreboxetine” [2016]. Their results indicated that after stopping cocaine use, an average of 3 wk passed before participants’ brains returned to baseline (Fig. 26). Imaging of the evolution of binding potential during recovery, then, indicates an important neural correlate of the profound changes in craving and self-control during the first weeks of abstinence.

Amyloid is a central molecule in AD, but it is not the only molecule. Villemagne et al. from Austin Health (Melbourne, Australia) and a consortium of Australian and Japanese researchers reported on “In vivo  $\tau$  imaging in AD” [36]. Figure 27 shows an early in-human study of various types of dementias with the novel  $^{18}\text{F}$ -THK523 tracer. This is only the beginning of tau protein imaging, an important abnormal protein in the diagnosis and treatment of AD.

Dr. Wagner often quoted Dag Hammarskjöld, former secretary general of the United Nations, who said “only he who keeps his eye fixed on the far horizon will find his right road.” I strongly believe that our neuroscience community and SNMMI are on the right path—we can see the direction in which we must go to pursue a cure for AD, help PD patients, and better understand behavioral disorders and psychiatric conditions.

*Satoshi Minoshima, MD, PhD  
University of Washington  
Seattle, WA*